

APPLICATION OF FRONTAL DRIVE PRINCIPLES  
TO STRATIFIED RESERVOIRS,

By

ELTON WAYNE ADAMS

Bachelor of Science

Oklahoma State University

Stillwater, Oklahoma

1962

Submitted to the Faculty of the Graduate School of  
the Oklahoma State University  
in partial fulfillment of the requirements  
for the degree of  
MASTER OF SCIENCE  
May, 1964

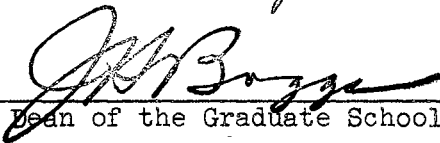
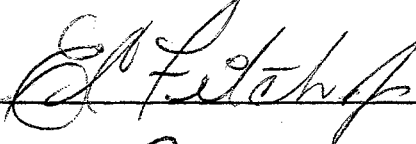
JAN 8 1965

APPLICATION OF FRONTAL DRIVE PRINCIPLES  
TO STRATIFIED RESERVOIRS

Thesis Approved:



\_\_\_\_\_  
Thesis Adviser



\_\_\_\_\_  
Dean of the Graduate School

570095

## ACKNOWLEDGEMENTS

I wish to express my sincere appreciation to the following for their roles in making this study possible:

To Professor A. G. Comer for his continuous advice and assistance during the past two years.

To my parents for their encouragement during my graduate study.

To Northern Natural Gas Company for their research sponsorship and to the staff of the Mechanical Engineering Department for the assistantship which made my graduate schooling possible.

To the personnel of the Underground Storage Department of Northern Natural Gas Company for their cooperation, especially Mr. A. I. Evernos.

To the personnel of both the Engineering Computer Laboratory and the University Computer Center.

To Lynn Boyd for his assistance in preparing drawings for this thesis.

To Dr. E. G. Woods for his contributions to my understanding of two-phase flow.

To Mrs. R. M. Schenandoah for typing this manuscript.

## TABLE OF CONTENTS

Chapter	Page
I. INTRODUCTION. . . . .	1
II. PREVIOUS INVESTIGATIONS . . . . .	3
III. THEORETICAL DEVELOPMENTS . . . . .	6
Water Flooding Application of Frontal Drive Theory . . . . .	6
Gas Storage in Stratified Aquifers . . . . .	17
IV. COMPUTER PROGRAMS . . . . .	25
Water Flooding. . . . .	25
A. Part One. . . . .	25
B. Part Two. . . . .	31
Gas Storage . . . . .	36
A. Part One. . . . .	37
B. Part Two. . . . .	46
C. Part Three. . . . .	46
V. EXAMPLE PROBLEMS AND RESULTS. . . . .	57
VI. SUMMARY AND CONCLUSIONS . . . . .	69
VII. RECOMMENDATIONS FOR FUTURE STUDY. . . . .	71
SELECTED BIBLIOGRAPHY. . . . .	73
APPENDIX . . . . .	75
List of Symbols for Text. . . . .	76

LIST OF TABLES

Table	Page
I. Frontal Drive Calculations for Water Flood. . . . .	26
II. Fortran Symbols for Water Flood Programs. . . . .	29
III. Water Flood Performance Calculations. . . . .	32
IV. Frontal Drive Calculations for Gas Injection. . . . .	38
V. Fortran Symbols for Gas Injection . . . . .	42
VI. Curve Fit for Frontal Drive Data . . . . .	47
VII. Gas Injection Performance Predictions . . . . .	49
VIII. Data for Water Flood Example. . . . .	58
IX. Two-Phase Flow Data, Case I . . . . .	62
X. Two-Phase, Stratification and Injection Data; Case I. . . . .	63
XI. Reservoir Performance, Case I . . . . .	64

## LIST OF FIGURES

Figure	Page
1. Typical Relative Permeability Curves. . . . .	7
2. Linear Displacement . . . . .	7
3. Typical Fractional Flow Curve . . . . .	10
4. Element of Porous Media Conducting Two-Phase Flow . . .	10
5. Tangent Method for Determining Frontal and Average Saturations . . . . .	13
6. Saturation Distribution . . . . .	13
7. Relative Permeability Distribution. . . . .	13
8. Linear Displacement in a Stratified System. . . . .	15
9. "Incompressible Core" . . . . .	18
10. A Two-Phase Flow Region . . . . .	20
11. Flow Chart of Part One Frontal Drive Water Flood Program . . . . .	27
12. Flow Chart of Part Two Frontal Drive Water Flood Program . . . . .	33
13. Flow Chart of Part One Gas Storage Program. . . . .	39
14. Flow Chart of Part Two Gas Storage Program. . . . .	48
15. Flow Chart of Part Three Gas Storage Program. . . . .	51
16. Comparison of Oil Production Rate Predictions . . . . .	59
17. Comparison of Oil Recovery Predictions . . . . .	60
18. Predicted Gas Zone Performance, Case I . . . . .	65
19. Predicted Gas Zone Performance, Case II . . . . .	67

Figure	Page
20. Distribution of Gas Among the Layers, Case I. . . . .	68
21. Distribution of Gas Among the Layers, Case II . . . . .	68

## CHAPTER I

### INTRODUCTION

When a fluid is injected into porous media to displace another fluid with which it is immiscible, two-phase flow occurs within the media. If the porous material is homogenous, the flow problem can be solved with the aid of experimental data. However, all natural formations are to some degree inhomogenous, i.e. permeability and porosity are not constant throughout. If the degree of inhomogeneity is great, the problem becomes almost impossible to solve analytically. A technique widely used to give approximate solutions to the problem consists of mathematically separating the formation into horizontal layers, strata, which are fairly homogenous within themselves. From this point, the problem may be handled in several ways depending upon the flowing fluids and the particular system which is to be described. Two examples of this problem are: 1) water flooding of oil from a reservoir; 2) storage of natural gas in an aquifer.

For many years the displacement of oil by water has been used to recover oil which could not have been produced by primary methods. In water flooding, fluid flow through any given portion of the reservoir is usually unidirectional because flow is always from injection wells to producing wells. Since a large capital outlay for equipment and operating expenses is required to water flood a reservoir it is quite desirable



to be able to predict in advance the performance of a given reservoir. One purpose of this thesis is to present an improved method of predicting water flood performances.

During the past decade the natural gas industry has begun storing gas in aquifers. A gas storage well is commonly used for both injection and withdrawal. Calculations are more difficult for the cyclic two-phase flow problem encountered in gas storage than for the unidirectional water flooding case. Relative permeability hysteresis and unsteady state flow account for much of the added complexity of the cyclic gas storage problem. It is very desirable to be able to predict the storage capacity and operating characteristics of an aquifer before millions of dollars are spent developing it into a storage facility. The main objective of this thesis is to combine techniques used in making water flood calculations with frontal drive and unsteady state flow relationships to obtain a method for predicting the performance of stratified gas storage reservoirs during injection.

## CHAPTER II

### PREVIOUS INVESTIGATIONS

Publications available on two-phase flow in porous media may be divided into three broad categories: 1) techniques for handling water flooding of homogenous and stratified reservoirs, 2) techniques describing the storage of natural gas in homogenous acquifers, 3) techniques describing oil displacement by gas drive. Only the first two categories were covered in this study.

Of the many proposed methods for predicting oil recovery by water flooding, probably the most widely known was published by Stiles (12)\* in 1948. His method utilizes the permeability distribution to divide the reservoir into layers. The chief assumptions of Stiles approach are: 1) a layered linear system is representative, 2) there is no cross-flow between the layers, 3) gravity and capillary effects are negligible, 4) all layers have the same porosity, 5) piston-like displacement occurs, and 6) the flow rate in each layer remains constant. A combination of the fourth and sixth assumptions indicates that the rate of advance of a flood front in a layer is directly proportional to its absolute permeability. In that case, the fraction of a layer swept by a flood front is merely the ratio of its absolute permeability

---

\*Note: Numbers in parentheses refer to references in Selected Bibliography.

to that of the layer just watered-out. Stiles used the ratio of permeabilities and the thicknesses of the layers to calculate fractional recovery.

In 1950, a method similar to that of Stiles was presented by Dykstra and Parsons. (7) Their method is somewhat more rigorous in as much as the flow rate and frontal advance rate in each layer is allowed to be dependent upon mobility ratio and the positions of the other flood fronts. The first five assumptions listed above were maintained in their approach. Pirson (11) has discussed the relationships involved in several techniques for handling water flooding problems.

Published reports on single-layer model studies by Dyes et al (6) and by Craig et al (5) have allowed water flood geometry to be taken into account by the introduction of a sweep efficiency factor. Both groups of investigators used x-ray shadow graphs to determine the swept areas. Dyes group studied several displacement patterns; including the five-spot, line drive, and staggered line drive. They used miscible fluids and had nearly piston-like displacement in their experiments. The published correlations by Craig's group are for the five-spot pattern in which water was used to displace an oil phase. In some cases an initial gas saturation existed. Craig concluded that the presence of an initial gas saturation has very little effect upon the sweep efficiency. Both groups used mobility as the principle parameter in their correlations.

Buckley and Leverett (2) have presented analytical relationships describing the simultaneous flow of two immiscible fluids in porous media. Their frontal drive equations describe the saturation distribution behind the flood front and do not imply piston-like displacement. Their developments indicate that the rate of frontal advance is proportional to the

derivative of fractional flow with respect to saturation. Fractional flow is dependent upon fluid viscosities and experimentally determined relative permeabilities.

The Buckley-Leverett relationships were made much more acceptable by Welge (13), who introduced a graphical technique which eliminates many tedious calculations. His method consists of drawing a tangent to the fractional flow versus saturation curve in order to determine frontal saturation and average saturation behind the front. The tangent method is in reality the application of a material balance relationship.

Woods and Comer (14) have applied the Buckley-Leverett frontal drive principles to gas storage in a homogenous radial aquifer. The method has been used to make predictions quite comparable to actual field results. Woods (15) has extended their method to cover the cyclic aspects of gas storage including relative permeability hysteresis. This author has extended and modified their work to cover injection in a stratified radial system surrounded by an infinite aquifer.

## CHAPTER III

### THEORETICAL DEVELOPMENTS

#### The Water Flooding Application of Frontal Drive Theory

As previously mentioned, many methods have been presented for predicting the water flood performance of stratified reservoirs. Common simplifying assumptions made in the derivation of these methods follow:

- 1) a non-homogenous reservoir may be mathematically represented by a layered linear system in which each layer is homogenous,
- 2) no cross-flow of fluid occurs between the layers,
- 3) gravitational and capillary pressure effects are negligible,
- 4) piston like displacement of the oil occurs, and
- 5) the layers have similar relative permeability characteristics which may be experimentally determined.

Relative permeabilities typically vary with saturation as shown in Figure 1. It is intended in this chapter to present a method for predicting water flood behavior in stratified reservoirs which does not include the fourth assumption. The assumption of piston-like displacement is eliminated by use of the Buckley-Leverett frontal drive theory.

The flow mechanics of a single layer system such as shown in Figure 2 will be analyzed before attacking a multi-layer system. Darcy's equation may be written for each of the flowing phases at any plane normal to the direction of flow.

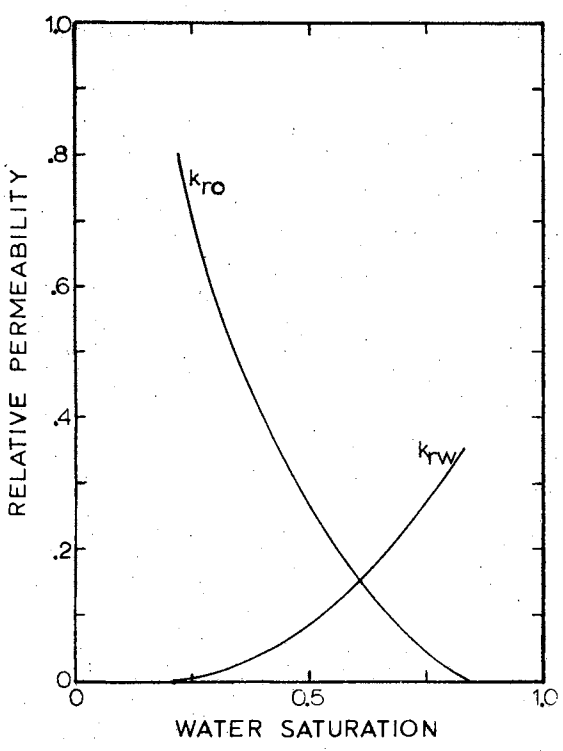


Figure 1. Typical Relative Permeability Curves.

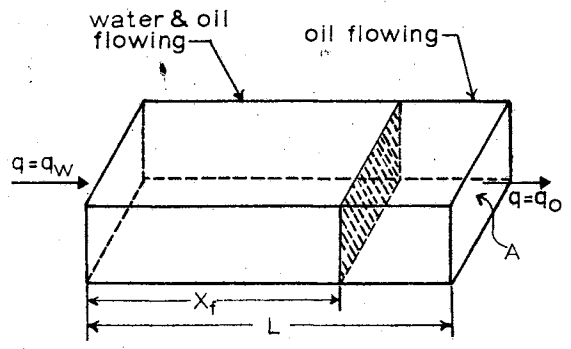


Figure 2. Linear Displacement.

$$q_w = - \frac{K_w A}{\mu_w} \left[ \frac{\partial P_w}{\partial X} + \rho_w g \sin \alpha \right] \tag{3-1}$$

$$q_o = - \frac{K_o A}{\mu_o} \left[ \frac{\partial P_o}{\partial X} + \rho_o g \sin \alpha \right] \tag{3-2}$$

For a definition of each symbol, please see the Appendix.

Capillary pressure is defined by

$$P_c = P_o - P_w \tag{3-3}$$

If all flow is assumed to occur in a horizontal direction and capillary pressure is negligible, Equations (3-1) and (3-2) may be simplified to the following forms.

$$q_w = - \frac{k_w A}{\mu_w} \frac{\partial p}{\partial X} \quad (3-4)$$

$$q_o = - \frac{k_o A}{\mu_w} \frac{\partial p}{\partial X} \quad (3-5)$$

The assumption of no vertical flow is well justified in reservoirs where vertical permeabilities are small in comparison with horizontal permeabilities. The occurrence of tight streaks in reservoirs also tends to validate the assumption of no vertical flow.

The fractional flow of water through any cross section is defined as

$$f_w = \frac{q_w}{q_w + q_o} \quad (3-6)$$

Upon the substitution of Equations (3-4) and (3-5), Equation (3-6) becomes

$$f_w = \frac{\frac{k_w}{\mu_w}}{\frac{k_w}{\mu_w} + \frac{k_o}{\mu_o}} \quad (3-7a)$$

or

$$f_w = \frac{1}{1 + \frac{k_o \mu_w}{k_w \mu_o}} \quad (3-7b)$$

Since the ratio of effective permeabilities is the same as the ratio of relative permeabilities, the fractional flow-saturation relationship can be calculated from experimental relative permeability data. A typical fractional flow-saturation relationship is shown in Figure 3.

A material balance may be applied to a thin segment of porous media as shown in Figure 4. The volume of oil initially in the section is

$$V_{oi} = S_{oi} \phi A \Delta x. \quad (3-8)$$

Assuming that the fluids are incompressible, a small increment of time later the volume of oil present in the segment is

$$V_{oi} - \Delta q_o \Delta t = S_o \phi A \Delta x. \quad (3-9)$$

Also

$$\Delta S_o = S_o - S_{oi} \quad (3-10)$$

$$-\Delta q_o \Delta t = S_o \phi A \Delta x - S_{oi} \phi A \Delta x \quad (3-11)$$

$$\frac{\Delta q_o}{\Delta x} = \phi A \frac{\Delta S_o}{\Delta t}. \quad (3-12)$$

Taking limits as  $\Delta x$  and  $\Delta t$  approach zero, one obtains

$$\frac{\partial q_o}{\partial x} = - \phi A \frac{\partial S_o}{\partial t}. \quad (3-13)$$



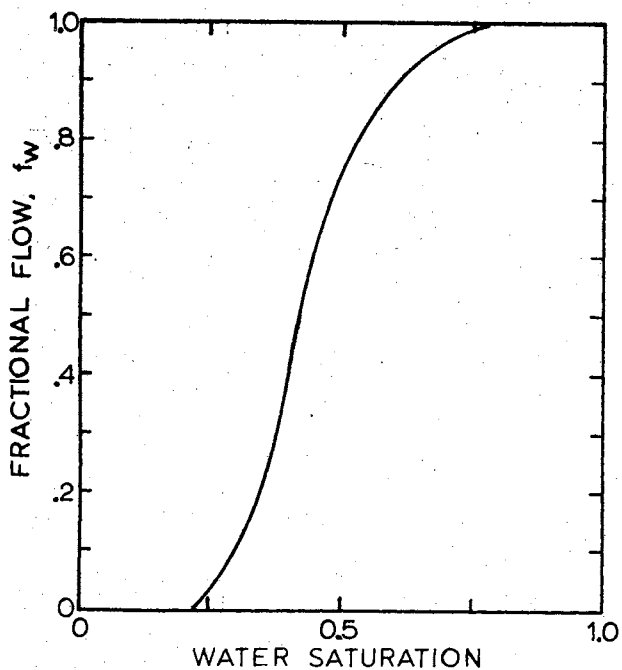


Figure 3. Typical Fractional Flow Curve.

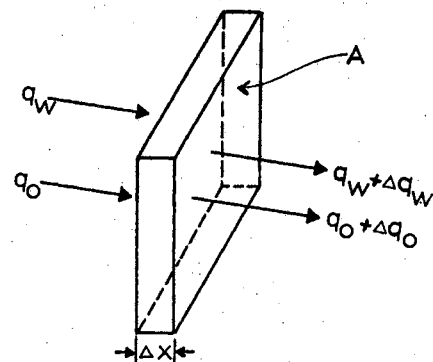


Figure 4. Element of Porous Media Conducting Two-Phase Flow.

A similar relationship may be obtained for water flow, only the subscripts need changing.

$$\frac{\partial q_w}{\partial x} = -\phi A \frac{\partial S_w}{\partial t} \quad (3-14)$$

Since the total flow rate does not vary with distance,

$$\frac{\partial q_w}{\partial x} = q \frac{\partial f_w}{\partial x} \quad (3-15)$$

where

$$q = q_o + q_w. \quad (3-16)$$

Equations (3-14) and (3-15) may be combined.

$$q \frac{\partial f_w}{\partial x} = - \varphi A \frac{\partial S_w}{\partial t} \quad (3-17)$$

If  $x$  is the distance to a plane of constant saturation, at that plane the total derivative of saturation as a function of time and distance is

$$\frac{dS_w}{dt} = \frac{\partial S_w}{\partial t} + \frac{\partial S_w}{\partial x} \frac{dx}{dt} = 0 \quad (3-18)$$

and

$$\frac{\partial f_w}{\partial x} = \frac{\partial f_w}{\partial S_w} \frac{\partial S_w}{\partial x} \quad (3-19)$$

Equations (3-17), (3-18) and (3-19) are now combined to relate displacement and time.

$$q \frac{\partial f_w}{\partial S_w} = \varphi A \frac{dx}{dt} \quad (3-20)$$

Separating variables and integrating at constant saturation yield

$$X_{(t)} - X_{(0)} = \frac{Q_{(t)} - Q_{(0)}}{\varphi A} \left( \frac{\partial f_w}{\partial S_w} \right)_S \quad (3-21)$$

where  $X$  is the displacement of a constant saturation  $S$  due to a cumulative fluid flow  $Q$ .

From the previously calculated fractional flow-saturation relationship, the derivatives of fractional flow with respect to saturation may

be obtained graphically or by numerical means such as the method of central differences. Through the use of Equation (3-21) it is possible to calculate the saturation distribution behind the flood front at any time. However, this calculation does not establish the saturation at the front.

Welge (13) has shown that if a tangent to the fractional flow versus saturation curve is drawn as in Figure 5, the saturation at the point of tangency is the saturation at the flood front. If the tangent is extended to a fractional flow of unity, the saturation at that point is the average saturation behind the flood front. The saturation distribution for a linear system would appear as shown in Figure 6.

Since saturations are known as a function of distance, relative permeabilities could be plotted as a function of distance and would appear as shown in Figure 7. The average relative permeability to each phase between the inlet face and any point behind the flood front may be determined by graphical integration or by numerical methods. Simpson's rule gives the following equation.

$$\bar{k}_r = \frac{\sum_{i=S_w}^{S_{wm}} (k_{r1} + k_{r1+1})(X_i - X_{i+1})}{X_{S_w}} \quad (3-22)$$

Where  $S_w$  is any water saturation behind the front and  $S_{wm}$  is the water saturation associated with residual oil saturation.

If the front has not yet reached the outlet face, the following equations may be used to determine the average relative permeabilities

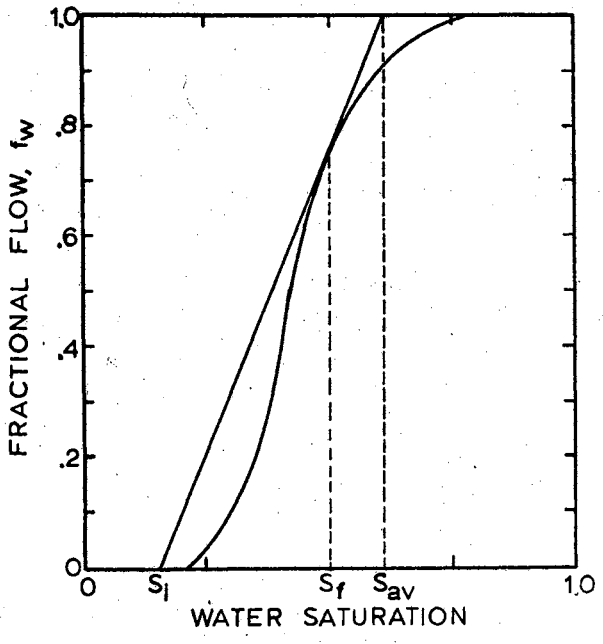


Figure 5. Tangent Method for Determining Frontal and Average Saturations.

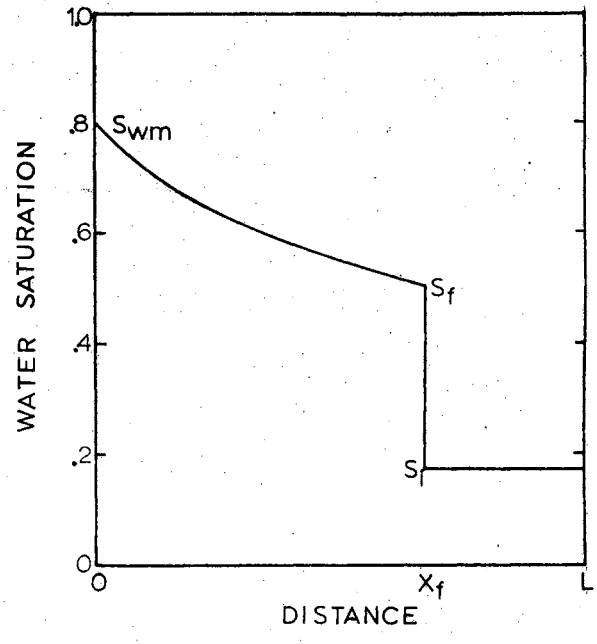


Figure 6. Saturation Distribution.

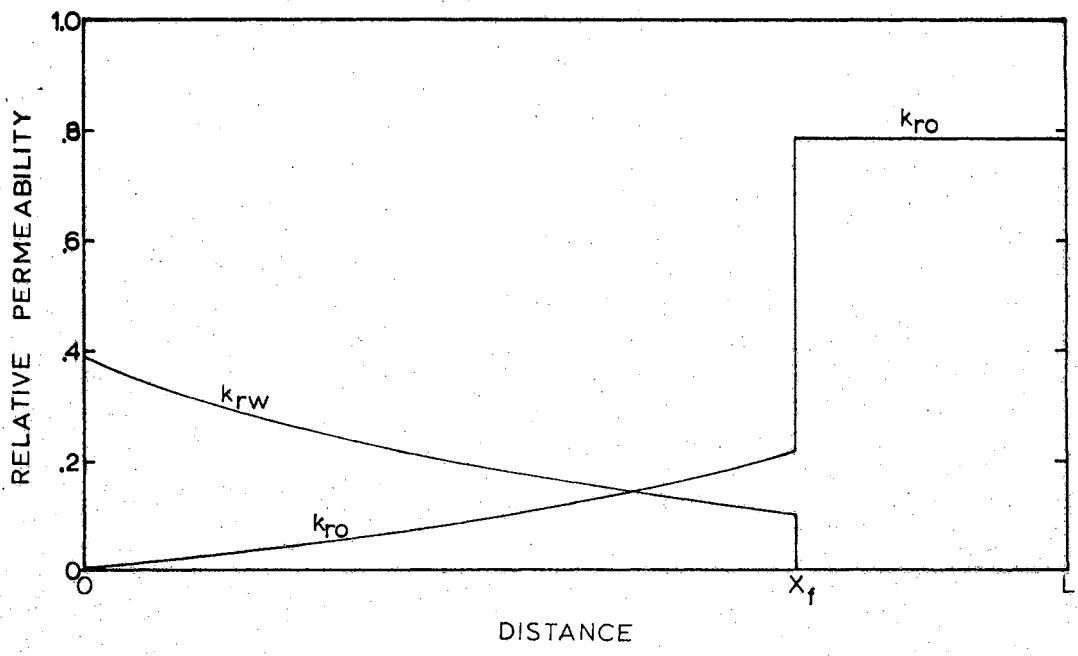


Figure 7. Relative Permeability Distribution.

over the entire length.

$$\bar{k}_{rw} = \frac{\sum_{i=S_{wf}}^{S_{wm}} (k_{rwi} + k_{rwi+1})(X_i - X_{i+1})}{2L} \quad (3-23)$$

$$\bar{k}_{ro} = \frac{k_{ro}(L - X_f) + \frac{1}{2} \sum_{i=S_{wf}}^{S_{wm}} (k_{roi} + k_{roi+1})(X_i - X_{i+1})}{L} \quad (3-24)$$

Figure 8 is the basic model from which many procedures for handling stratified reservoirs are developed. The expressions previously obtained are to be applied to each individual layer.

Darcy's equation may be written for each layer.

$$q_1 = K_1 \left( \frac{\bar{k}_{ro}}{\mu_o} + \frac{\bar{k}_{rg}}{\mu_g} \right)_1 \frac{Wh_1 \Delta P_1}{L} \quad (3-25a)$$

$$q_2 = K_2 \left( \frac{\bar{k}_{ro}}{\mu_r} + \frac{\bar{k}_{rg}}{\mu_g} \right)_2 \frac{Wh_2 \Delta P_2}{L} \quad (3-25b)$$

$$q_3 = K_3 \left( \frac{\bar{k}_{ro}}{\mu_o} + \frac{\bar{k}_{rg}}{\mu_g} \right)_3 \frac{Wh_3 \Delta P_3}{L} \quad (3-25c)$$

The relative mobility for a layer may be defined as

$$\bar{M} = \frac{\bar{k}_{ro}}{\mu_o} + \frac{\bar{k}_{rw}}{\mu_w} \quad (3-26)$$

The pressures differential may be assumed equal across all layers,

$$\frac{Lq_1}{Wh_1K_1\bar{M}_1} = \frac{Lq_2}{Wh_2K_2\bar{M}_2} = \frac{Lq_3}{Wh_3K_3\bar{M}_3} \quad (3-27)$$

$$\frac{q_1}{h_1K_1\bar{M}_1} = \frac{q_2}{h_2K_2\bar{M}_2} \quad (3-28)$$

$$\frac{q_1}{h_1K_1\bar{M}_1} = \frac{q_3}{h_3K_3\bar{M}_3} \quad (3-29)$$

$$q = q_1 + q_2 + q_3 \quad (3-30)$$

When the total flow rate is known, Equations (3-28), (3-29) and (3-30) may be solved simultaneously for the individual flow rates.

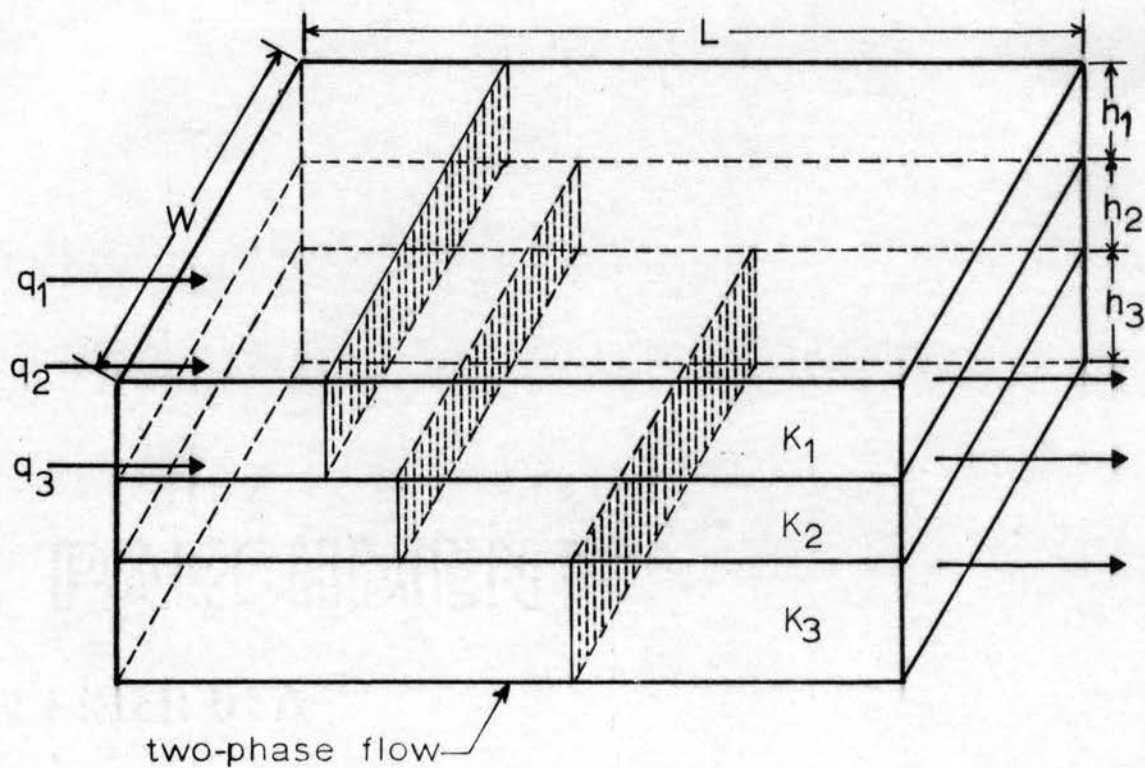


Figure 8. Linear Displacement in a Stratified System.

$$q_1 = \frac{q h_1 K_1 \bar{M}_1}{h_1 K_1 \bar{M}_1 + h_2 K_2 \bar{M}_2 + h_3 K_3 \bar{M}_3} \quad (3-31a)$$

$$q_2 = \frac{q h_2 K_2 \bar{M}_2}{h_1 K_1 \bar{M}_1 + h_2 K_2 \bar{M}_2 + h_3 K_3 \bar{M}_3} \quad (3-31b)$$

$$q_3 = \frac{q h_3 K_3 \bar{M}_3}{h_1 K_1 \bar{M}_1 + h_2 K_2 \bar{M}_2 + h_3 K_3 \bar{M}_3} \quad (3-31c)$$

More generally, the division of flow among the layers of a stratified system is given by

$$q_j = \frac{q h_j K_j \bar{M}_j}{\sum_{j=1}^N h_j K_j \bar{M}_j} \quad (3-32)$$

The relative flow rates through the layers vary as the flood fronts move, making it quite difficult to rigorously obtain an expression for the cumulative flow through each layer. However, the flow rates through the beds may be assumed constant for a short period of time and summations of the cumulative flows for many time steps may be made. Knowing the cumulative total flow through a layer, the saturation at its outlet may be determined. When the outlet saturations are known the fractional flow from each layer may be calculated by Equation (3-7b).

The fractional flow of water from the combined system at any time is determined by

$$F_w = \frac{1}{q} \left[ f_{w1} q_1 + f_{w2} q_2 + \dots + f_{wN} q_N \right] \quad (3-33)$$

Equation (3-33) gives the combined fractional flow at reservoir conditions. The fractional flow at surface conditions may be obtained from the following expression.

$$F_{ws} = \frac{B_o F_w}{F_w (B_o - 1) + 1} \quad (3-34)$$

To manually calculate the predicted water flood performance of a reservoir from the relations given in this chapter would be an enormous task. Computer programs to execute the necessary calculations are presented in Chapter IV. Predictions by this method are compared to predictions by other methods in Chapter V.

#### Gas Storage in Stratified Aquifers

As previously reported, Woods and Comer (14) have developed and presented a method which quite accurately predicts the well bore pressure and radius of the gas zone for gas storage in relatively homogenous aquifers. Woods (15) has extended the method to include cyclic effects. Their method is to be modified and expanded to make predictions of well bore pressure and gas zone radii for injection into stratified reservoirs.

The mathematical model to be used to simulate a stratified storage reservoir is shown in Figure 9. Assumptions to be incorporated in this approach include: 1) compressibility of the formation and water may be neglected inside a finite region to be called the "incompressible core", 2) no cross-flow occurs between the layers within the "incompressible core, 3) the layers have similar relative permeability characteristics,



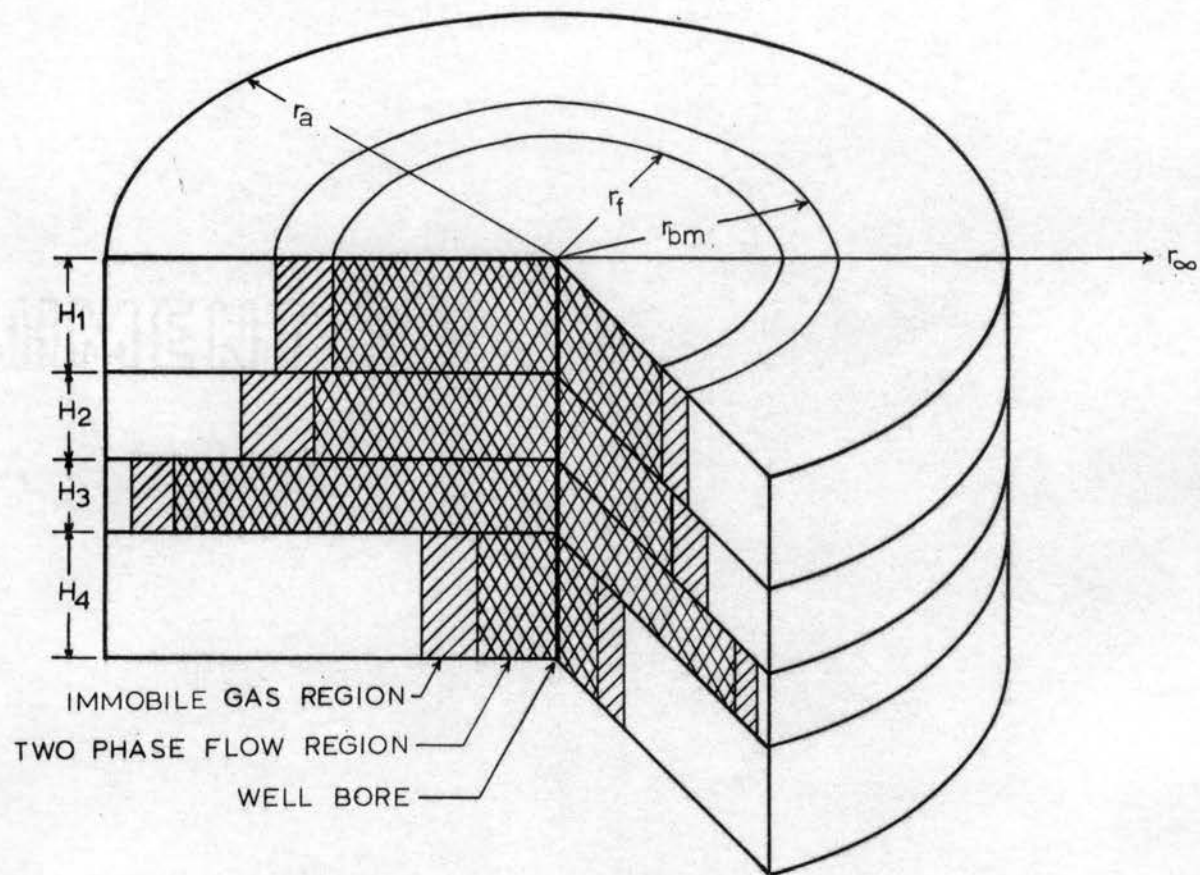


Figure 9. "Incompressible Core".

4) capillary and gravitational effects are negligible.

It has been shown that if capillary pressure and gravity effects are neglected, the fractional flow of gas at any saturation within a two-phase flow region may be calculated from experimental relative permeability data by the following expression.

$$f_g = \frac{1}{1 + \frac{k_{rw} \mu_g}{k_{rg} \mu_w}} \quad (3-35)$$

The derivative of fractional flow with respect to saturation versus saturation relationship may be determined numerically from the fractional flow saturation relationship. The frontal saturation and average saturation behind the front may be obtained by Welge's tangent method.

It has also been shown that for radial two-phase flow in one layer

$$r_s^2 - r_w^2 = \frac{1}{\pi h \phi} \left( \frac{\partial f}{\partial S} \right)_S \int_0^t q(t) dt. \quad (3-36)$$

If Equation (3-36) is divided by itself evaluated at the frontal saturation several factors may be eliminated.

$$\frac{r_s^2 - r_w^2}{r_f^2 - r_w^2} = \frac{\left( \frac{\partial f}{\partial S} \right)_S}{\left( \frac{\partial f}{\partial S} \right)_{S_f}} \quad (3-37)$$

Since the well bore radius is normally small in comparison to the other radii, the dimensionless radius of a constant saturation may be approximated by

$$R_d = \frac{r_s}{r_f} \approx \left[ \frac{\left( \frac{\partial f}{\partial S} \right)_S}{\left( \frac{\partial f}{\partial S} \right)_{S_f}} \right]^{\frac{1}{2}}. \quad (3-38)$$

The pressure change across the two-phase flow region in any layer may be obtained by first dividing that region into many concentric cylindrical shells. In Figure 10 the number of shells has been reduced

for simplicity. The total fluid flow rate is assumed the same at all radii within the region. The pressure drop across the two-phase flow region is quite small in comparison with the absolute pressure existing in storage reservoirs. Therefore, the difference between total flow rates at the inside and outside of the two-phase region due to gas expansion is very small. Darcy's equation for radial incompressible flow may be applied to the cylindrical shells.

$$\Delta P_{TP} = \frac{25.11 q}{h K} \left[ \frac{\text{Ln} \left( \frac{r_1}{r_w} \right)}{\bar{M}_1} + \frac{\text{Ln} \left( \frac{r_2}{r_1} \right)}{\bar{M}_2} + \dots + \frac{\text{Ln} \left( \frac{r_f}{r_{f-1}} \right)}{\bar{M}_f} \right]$$

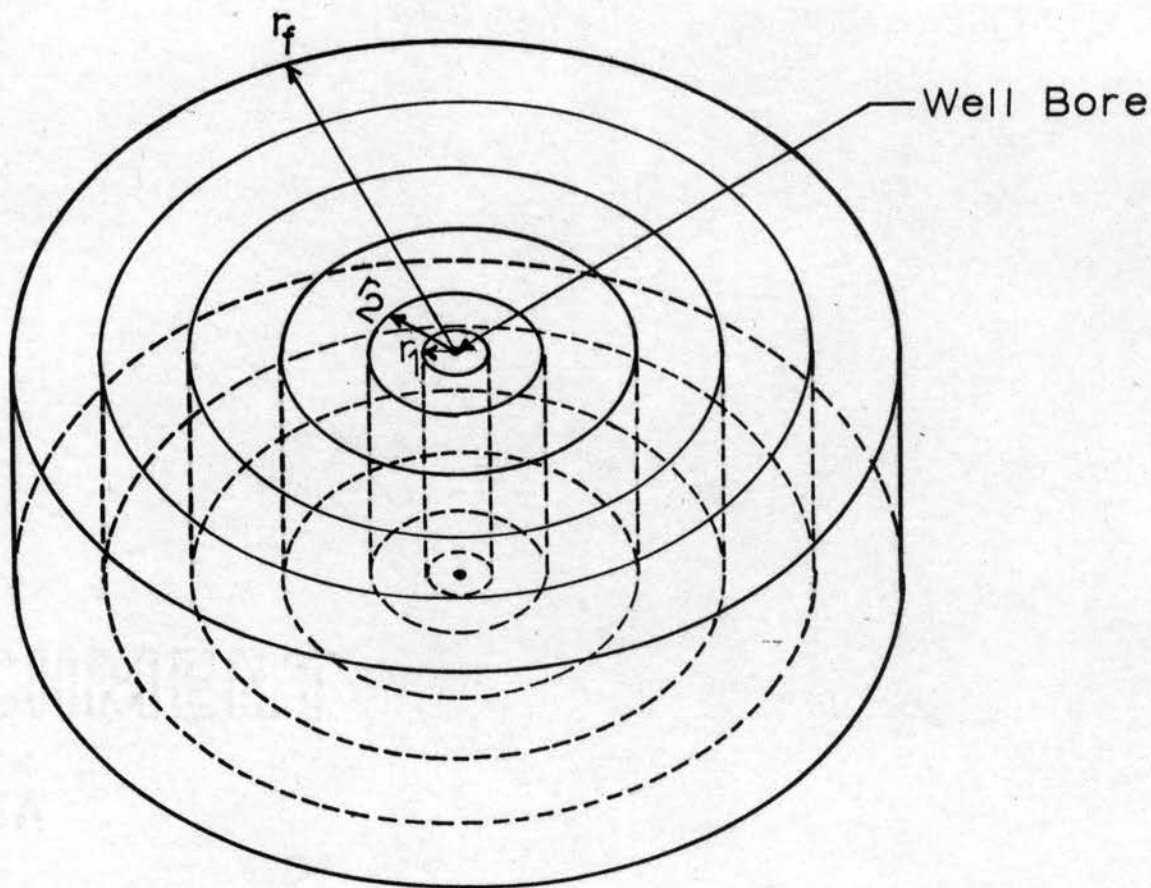


Figure 10. A Two-Phase Flow Region.

The average total relative fluid mobility for each cylindrical shell may be approximated by

$$\bar{M}_i \approx \frac{1}{2} \left[ \left( \frac{k_{rg}}{\mu_g} + \frac{k_{rw}}{\mu_w} \right)_{i-1} + \left( \frac{k_{rg}}{\mu_g} + \frac{k_{rw}}{\mu_w} \right)_i \right] \quad (3-40)$$

All the terms of the series portion of Equation (3-39) may be evaluated by using dimensionless radii except the first term, which requires that the radius of the two-phase flow zone be known. Therefore, the value of the series portion of that equation may be determined for any layer or gas zone radius simply by calculating the first term and combining it with the previously calculated value of the other terms. The entire series should be re-calculated if a large pressure change occurs because the mobilities and dimensionless radii are effected by changes in the pressure dependent gas viscosity.

The pressure differential across the portion of a layer in which only water flows is given by

$$\Delta P_w = \frac{25.11 q \mu_w}{h K} \left[ \text{Ln} \left( \frac{r_a}{r_{bm}} \right) + \frac{1}{k_{rw}} \text{Ln} \left( \frac{r_{bm}}{r_f} \right) \right] \quad (3-41)$$

where  $k_{rw}$  is evaluated at the saturation of the immobile gas region. If no immobile gas region exists, the last term becomes zero.

The unsteady state pressure change at the exterior of the "incompressible core" is to be determined for the case in which the surrounding aquifer is essentially infinite in lateral extent. Woods and Comer have

accomplished this by applying the work of Van Everdingen and Hurst. However, the exponential integral solution of the diffusivity equation is applicable and somewhat easier to evaluate. (3, 4)

$$\Delta P_{us} = p_a - p_e = q_d \text{Ei}(t_d) \quad (3-42)$$

where dimensionless time and pseudo-dimensionless flow rate are defined as follows:

$$t_d = \frac{-39.5 \mu_a \varphi_a C r_a^2}{K_a t} \quad (3-43)$$

$$q_d = \frac{-(1.258 \times 10^{-5}) q \mu_w}{K_a h_a} \quad (3-44)$$

The unsteady state pressure change for a series of constant flow rates is given by

$$\Delta P_{us} = q_{d1} \text{Ei}(t_{d1}) + (q_{d2} - q_{d1}) \text{Ei}(t_{d2}) + (q_{d3} - q_{d2}) \text{Ei}(t_{d3}) + \dots \quad (3-45)$$

The well bore pressure at any time is given by

$$p_w = p_e + \Delta P_{us} + \Delta P_w + \Delta P_{tp} \quad (3-46)$$

The pressure drop across the "incompressible core" may be calculated by combining Equations (3-39) and (3-41).

$$\Delta P_{ic} = \frac{25.11 q_j}{h_j K_j} \left[ R_{tp} + \mu_w \ln\left(\frac{r_a}{r_{bm}}\right) + \frac{\mu_w}{k_{rw}} \ln\left(\frac{r_{bm}}{r_f}\right) \right] \quad (3-47)$$

$$R_{tp} = \frac{\text{Ln}\left(\frac{r_1}{r_w}\right)}{M_1} + \frac{\text{Ln}\left(\frac{r_2}{r_1}\right)}{M_2} + \dots + \frac{\text{Ln}\left(\frac{r_f}{r_{f-1}}\right)}{M_f} \quad (3-48)$$

If the pressure drop across all layers is the same, the division of flow among the layers is given by

$$\frac{q_j}{q} = \frac{h_j K_j}{R_j \sum_{j=1}^N \frac{h_j K_j}{R_j}} \quad (3-49)$$

where

$$R_j = \left[ R_{tp} + \mu_w \text{Ln}\left(\frac{r_a}{r_{bm}}\right) + \frac{\mu_w}{k_{rw}} \text{Ln}\left(\frac{r_{bm}}{r_f}\right) \right]_j \quad (3-50)$$

The cumulative amount of gas injected in each layer can be determined by summing the amounts injected during a series of time steps. Upon knowing the cumulative injection into a layer and the saturation distribution, the radius of the two-phase flow region in that layer may be volumetrically determined.

The amount of gas in a layer is

$$Q_j = \frac{T_{sc} p \pi h_j \phi_j}{p_{sc} T Z} \left[ (\bar{s}_g - s_{gi}) r_f^2 + s_{gi} r_{bm}^2 \right]_j \quad (3-51)$$

Rearranging, Equation (3-51) becomes

$$r_f = \left[ \frac{1}{\bar{s}_g - s_{gi}} \left( \frac{Q_j p_{sc} T Z}{\pi h_j \phi_j T_{sc} p} - s_{gi} r_{bmj}^2 \right) \right]^{\frac{1}{2}} \quad (3-52)$$

A survey of the equations given in this section reveals that in order to calculate reservoir flow rates the well bore pressure must be known. To calculate the well bore pressure one must know the reservoir flow rates. Therefore, it is not possible to make direct calculations of either. An iterative solution is required. Computer programs to make pressure and radii predictions are given in Chapter IV. An example problem for a three-layer reservoir is given in Chapter V.

## CHAPTER IV

### COMPUTER PROGRAMS

In order to eliminate the tedious hand calculations that would be required to solve the expressions given in Chapter III, two sets of computer programs were written. One set was written for water flood calculations, the other for gas storage. All programs were written in Fortran language.

#### Water Flooding

First an attempt was made to write one program for all the required calculations. However it was necessary to divide the calculations into two sections due to the limited storage of the IBM 1620 computer available.

A. Part One. The first program was written to calculate basic frontal drive data. A listing of that program is given in Table I and its flow chart is shown in Figure 11. A list of Fortran symbols used in the water flood programs is given in Table II.

The first program requires as input data: 1) oil viscosity, 2) water viscosity, 3) oil formation volume factor, 4) water injection rate, 5) connate water saturation, 6) initial gas saturation, 7) bulk volume of the reservoir, 8) pattern or sweep efficiency, 9) return efficiency, 10) water cut at abandonment, 11) lowest saturation at



TABLE I

## FRONTAL DRIVE CALCULATIONS FOR WATER FLOOD

C	FRONTAL DRIVE WATERFLOOD IN A STRATIFIED RESERVOIR	001
C	PART 1, CALCULATION OF ESSENTIAL FRONTAL DRIVE DATA	002
	DIMENSION RKO(100),RKW(100),FW(100),DFW(100),SAV(100),ROB(100)	003
	DIMENSION RWB(100)	0 4
1	READ,VO,VW,BO,WIR,CW,SG,BV,SE,E,CUT,IL,IU	005
C	LET I RANGE FROM IL-2 TO IU+2	006
2	READ,I,RKO(I),RKW(I)	0 7
	FW(I)=(RKW(I)*VO)/((VO*RKW(I))+(RKO(I)*VW))	008
	IF (IU+2-I)3,3,2	0 9
3	DO 4 I=IL,IU	010
4	DFW(I)=(FW(I-2)-FW(I+2)+(8.*(FW(I+1)-FW(I-1))))/.12	011
	ICW=CW+.5	012
	IF (ICW-IL)6,6,5	013
5	ICW=IL	014
6	B=ICW	015
	SLO=0.	016
	L=IL+2	017
	DO 8 I=L,IU	018
	A=I	019
	SL=FW(I)/(A-B)	020
	IF (SLO-SL)7,8,8	021
7	SFA=I	022
	SLO=SL	023
8	CONTINUE	024
	K=SFA	025
	C=DFW(K)	026
	TYPE,SFA,IU	027
	PUNCH,SFA,SLO,C	028
	IF (K-IU)10,9,9	029
9	STOP	030
10	SP=0.	031
	SPW=0.	032
	ROB(I)=0.	033
	RWB(I)=RKW(I)	034
	X=0.	035
11	I=I-1	036
	XS=DFW(I)/C	037
	PO=.5*(RKO(I)+RKO(I+1))*(XS-X)	038
	PW=.5*(RKW(I)+RKW(I+1))*(XS-X)	039
	SP=SP+PO	040
	SPW=SPW+PW	041
	ROB(I)=SP/XS	042
	RWB(I)=SPW/XS	043
	X=XS	044
	IF (I-K)12,11,11	045
12	L=IU-1	046
	DO 13 I=K,L	047
	A=I	048
	SAV(I)=A+((100.*(1.-FW(I)))/DFW(I))	049
	PUNCH,I,SAV(I),ROB(I),RWB(I),I,FW(I),DFW(I)	050
13	CONTINUE	051
	I=IU	052
	SAV(IU)=IU	053
	PUNCH,I,SAV(I),ROB(I),RWB(I),I,FW(I),DFW(I)	054
	GO TO 1	055
	END	056

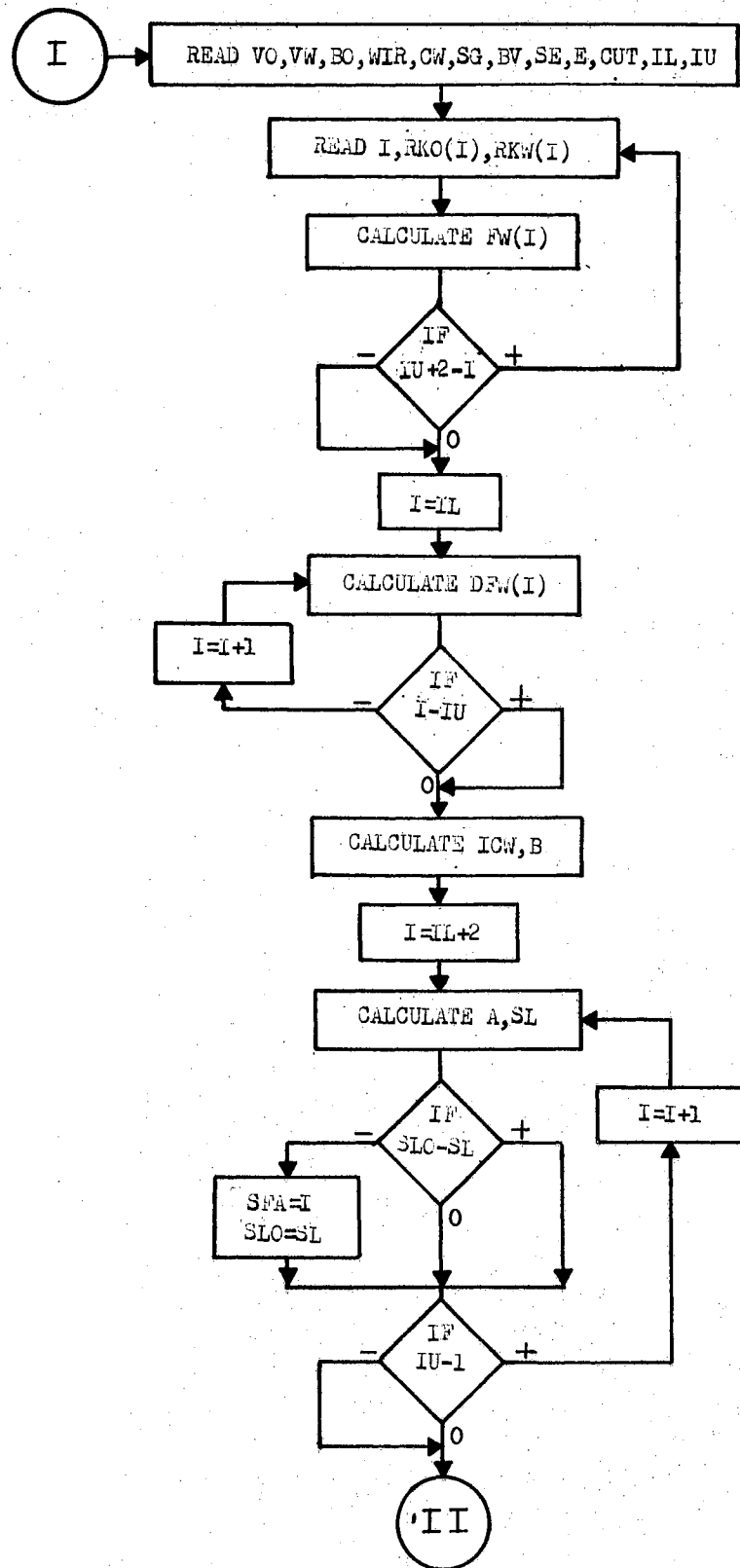


Figure 11. Flow Chart of Part One Frontal Drive Water Flood Program.

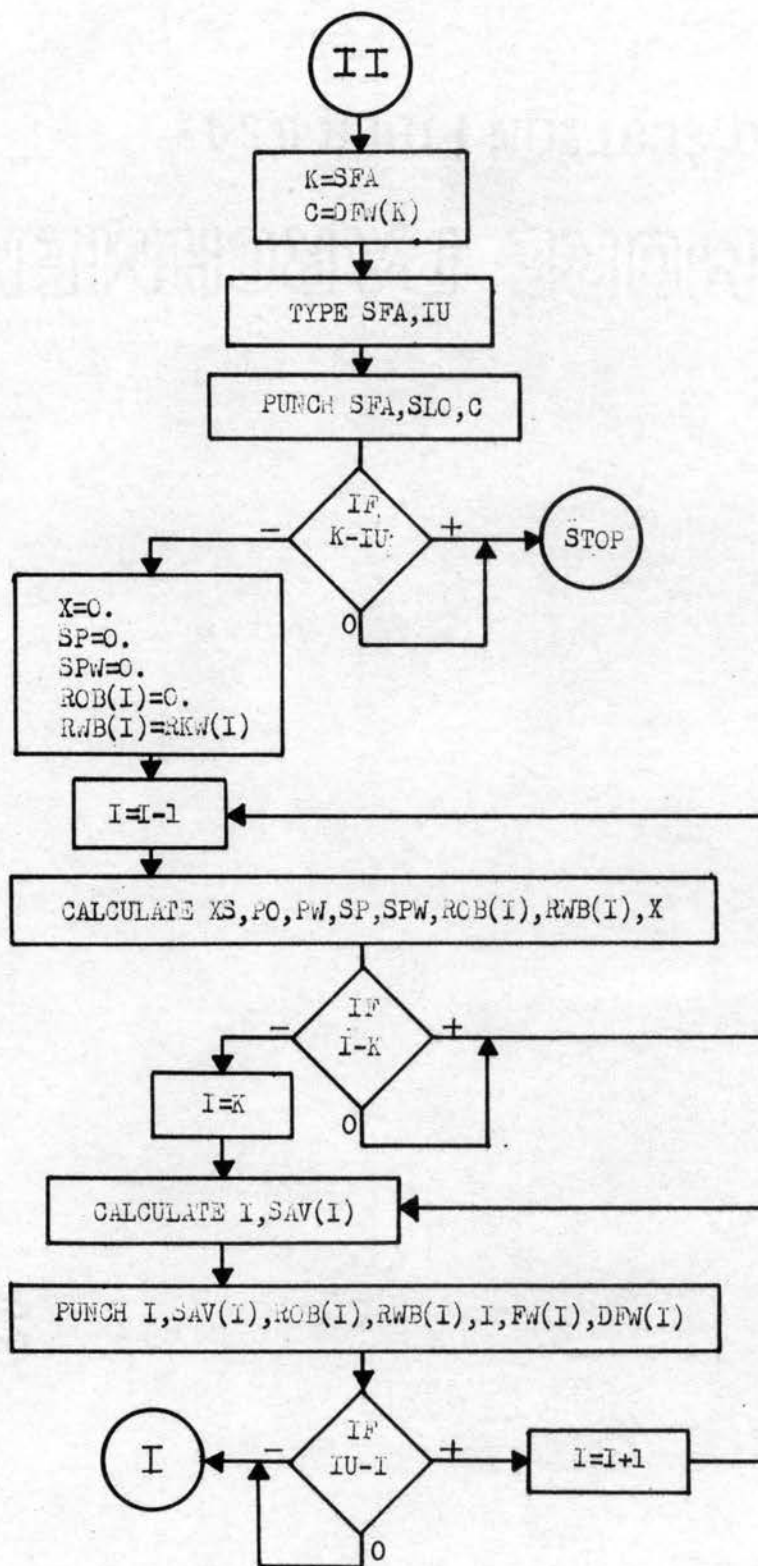


Figure 11. (Continued)

TABLE II

## FORTRAN SYMBOLS FOR WATER FLOOD PROGRAMS

BV	Bulk volume of reservoir being flooded, acre-ft.
BK(J)	Average base permeability of layer, J, md.
BO	Oil formation volume factor, res. vol./stock tank vol.
C	Derivative of fractional flow with respect to saturation taken at the flood front.
CUT	Producing water cut at abandonment, fractional.
CW	Connate water saturation, percent.
DFW(I)	Derivative of fractional flow with respect to saturation taken at water saturation I.
DFW(1)	Derivative of fractional flow at the outlet of a layer which has been swept by a flood front.
DFW(2)	Dummy variable used in determining the outflow saturation of a layer which has been swept by a flood front.
DFW(3)	Used similarly to DFW(2).
DT	Time step, days.
E	Return efficiency, Injection rate/total production rate.
FW(I)	Fractional flow of water at water saturation I.
H(J)	Thickness of layer J, feet.
HKT	Summation of capacities of all layers, md.-ft.
HT	Total thickness of all layers.
I	Water saturation, percent.
ICW	Connate water saturation in fixed point form, percent.
IL	Water saturation below which water cannot flow, percent.
IU	Water saturation above which oil cannot flow, percent.
J	Fixed point variable used to designate the layers.
K	Water saturation at the flood fronts, percent.
M	Dummy variable used for programming purposes only.
P(J)	Porosity of layer J, percent
Q(J)	Injection rate into layer J, barrels/day.
QO	Oil production rate, STB/day.
R	Unit recovery factor, STB/ac.-ft.
RKO(I)	Relative permeability to oil at water saturation I.

TABLE II(Continued)

RKW(I)	Relative permeability to water at saturation I.
RO	Average relative permeability to oil behind the flood front.
ROB(I)	Average relative permeability to oil behind saturation I.
ROC	Relative permeability to oil at connate water saturation.
RW	Average relative permeability to water behind the flood front.
RWB(I)	Average relative permeability to water behind saturation I.
SAV(I)	Average water saturation behind saturation I.
SE	Sweep efficiency, fractional.
SFA	Water saturation at the fronts, percent.
SG	Gas saturation before flooding, percent.
SLO	Slope of a tangent to the fractional flow vs. saturation curve at frontal saturation.
SL	Dummy variable used in determining SLO.
SM(J)	Average total relative fluid mobility in layer J.
SO	Average oil saturation of the reservoir, percent.
SP	Summation of relative permeabilities to oil.
SPW	Summation of relative permeabilities to water.
T	Time since water injection began, days.
TFW	Producing water cut at surface conditions at the end of the time step, fractional.
VO	Viscosity of oil in the reservoir, centipoise.
VW	Viscosity of water in the reservoir, centipoise.
WI	Cumulative water injected, barrels.
WIR	Water injection rate, barrels/day.
X	Dimensionless distance to water saturation I+1.
XS	Dimensionless distance to water saturation I.
Z(J)	Fraction of layer J which is behind the flood front.
ZP	Fraction of layer 1 behind the flood front at the end of the time step.

which water can flow, 12) highest water saturation at which oil can flow, 13) a table of relative permeabilities to oil and water with corresponding saturations. The input data is called for by Cards 5 and 7 of the program listing.

The Fortran statement on Card 8, a form of Equation (3-7) is used to calculate fractional flow of water at each 1% saturation interval. The statement on Card 11 calculates derivatives of fractional flow with respect to saturation numerically by a central differences technique. The calculations by Cards 12 through 26 are equivalent to drawing a tangent to the fractional flow curve to determine frontal saturation. In the event frontal saturation is calculated to be the saturation at which only residual oil exists, the computer stops. In that case, a method which assumes piston-like displacement could be used.

The punched output data from this program consists of: 1) frontal saturation, 2) slope of the tangent to the fractional flow curve, 3) a table giving average water saturation and average relative permeabilities behind any saturation, 4) a table of values of fractional flow and its derivatives with the corresponding water saturations.

B. Part Two. The second program applies the two-phase flow data which was calculated in Part One to a stratified system. Fortran statements for the second program are listed in Table III and its flow chart is shown in Figure 12. Input data required for the second program are: 1) oil viscosity, 2) water viscosity, 3) oil formation volume factor, 4) water injection rate, 5) connate water saturation, 6) initial gas saturation, 7) bulk volume of the reservoir, 8) horizontal sweep efficiency 9) return efficiency, 10) producing water cut at abandonment,



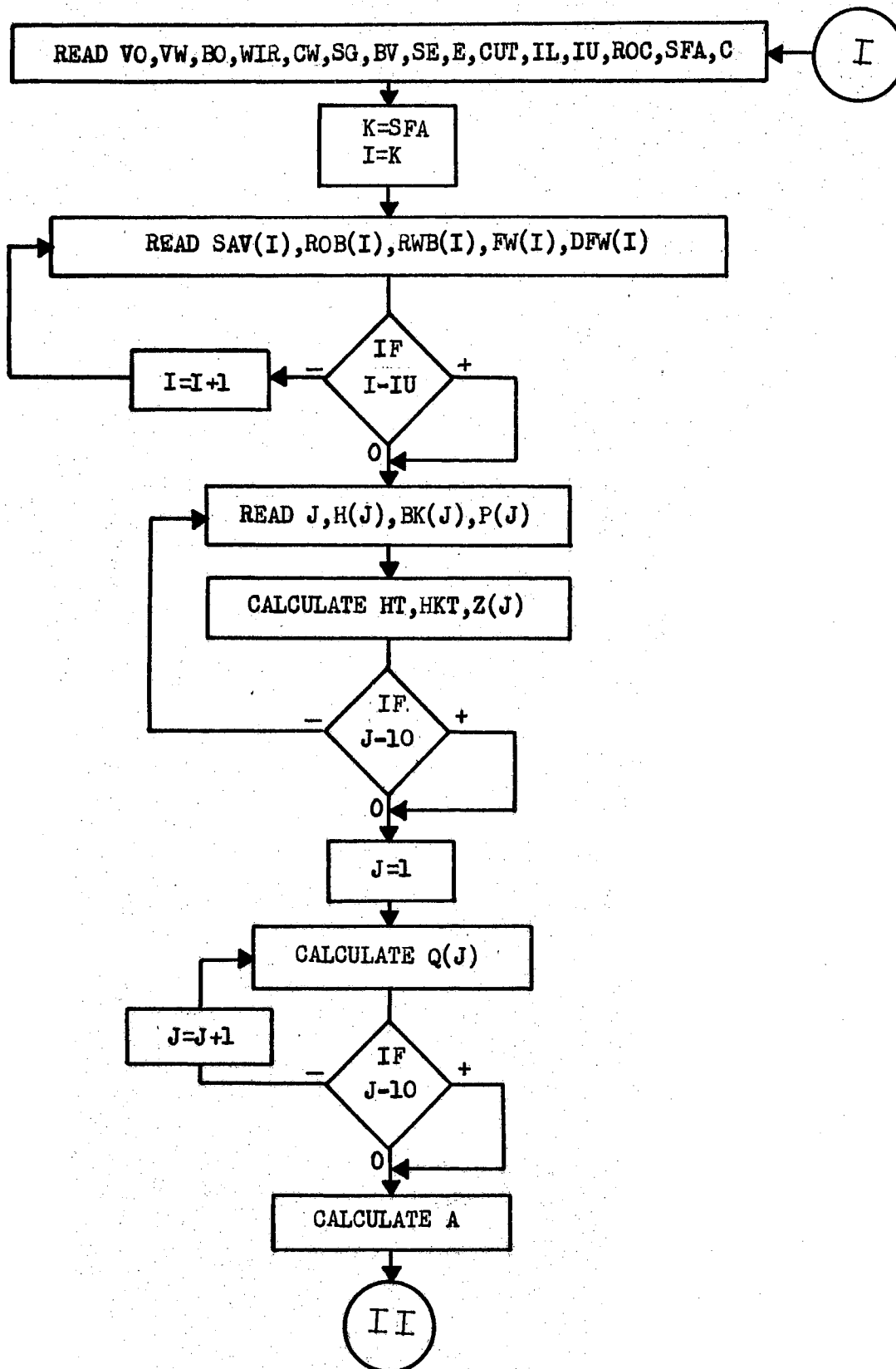


Figure 12. Flow Chart of Part Two Frontal Drive Water Flood Program.



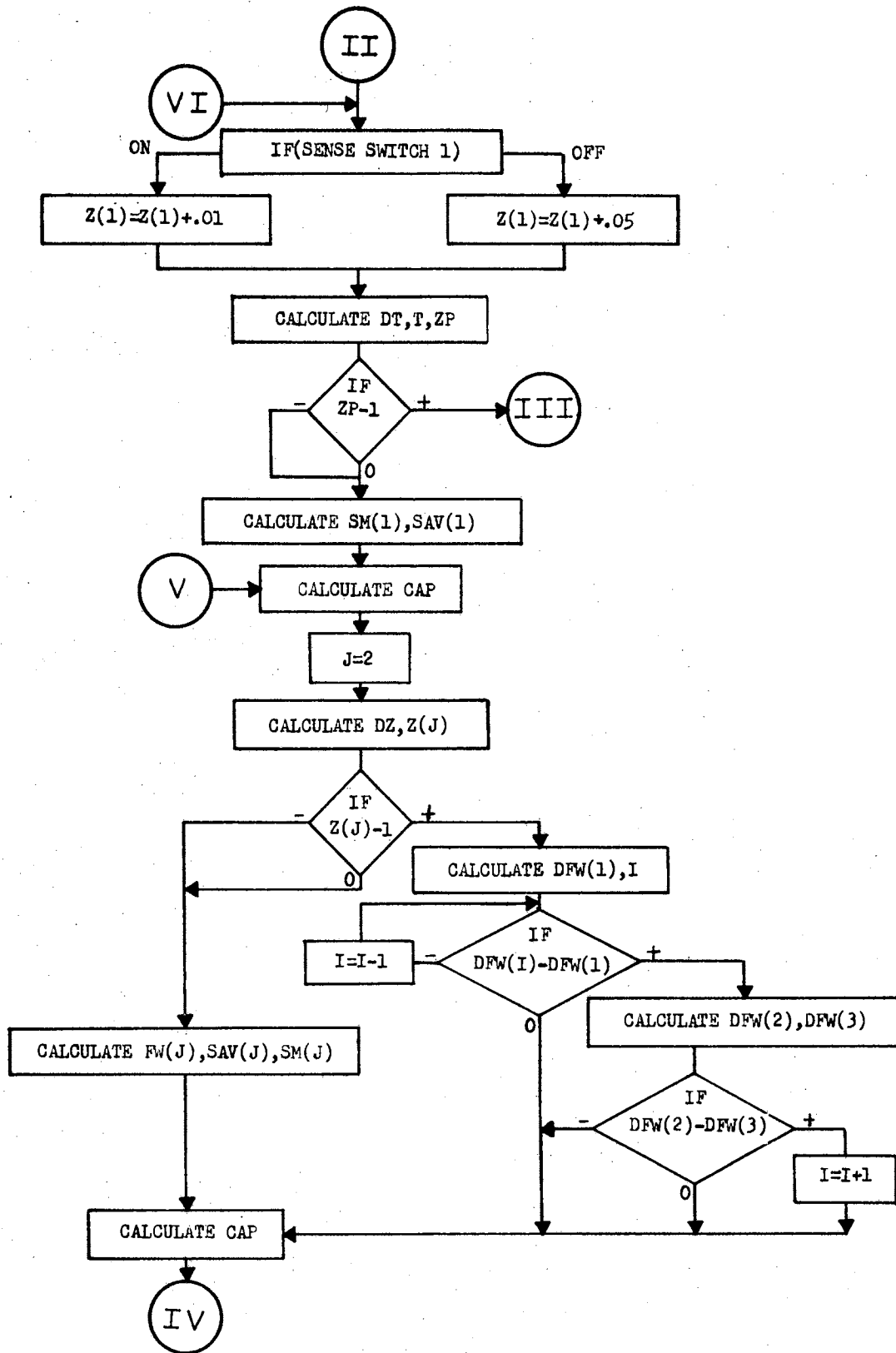


Figure 12. (Continued)

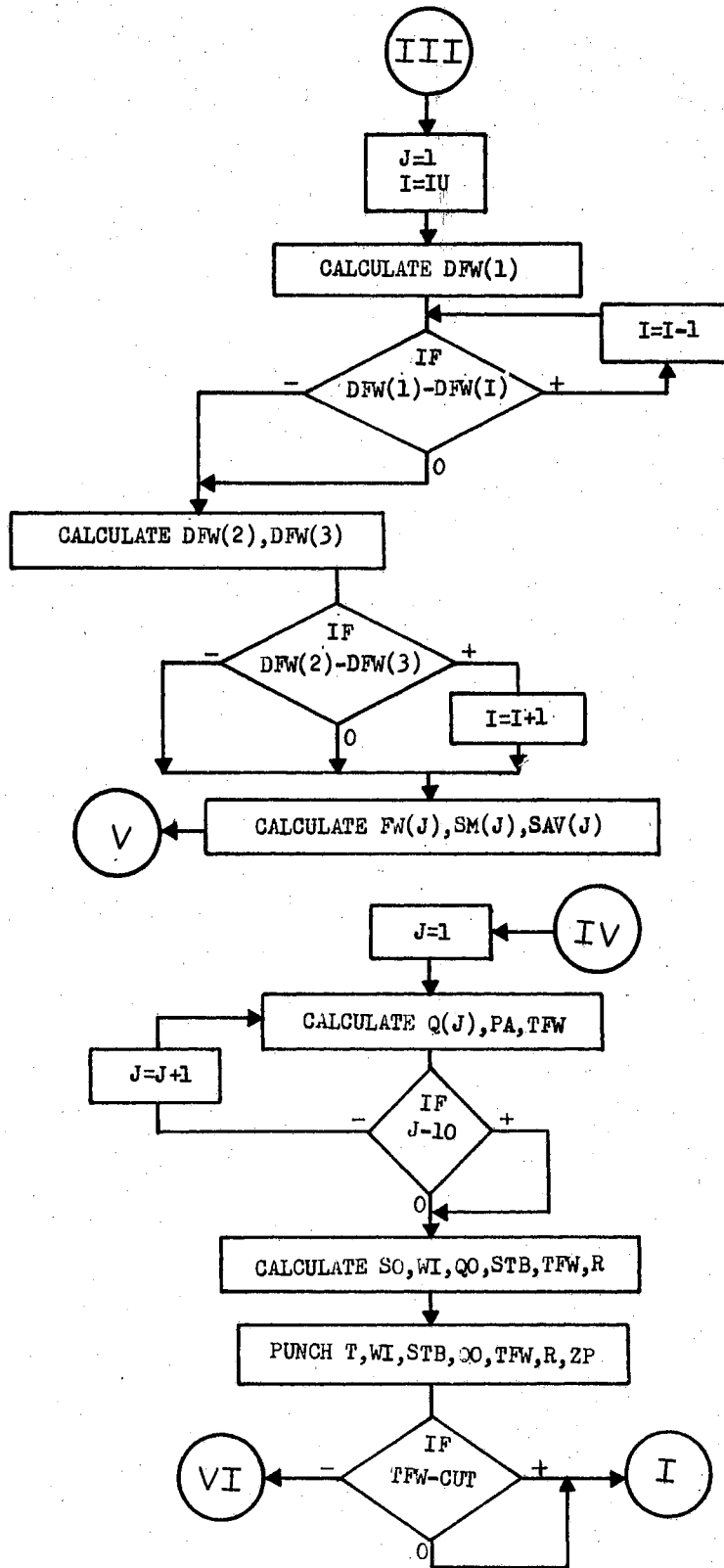


Figure 12. (Continued)

11) lowest saturation at which water can flow, 12) highest water saturation at which oil can flow, 13) relative permeability to oil at connate water saturation, 14) frontal saturation, 15) the table of average saturations and relative permeabilities from program one, and 16) the permeability, thickness, and porosity of each layer.

As the flood fronts advance at varying rates in the layers, the fraction of injected fluid entering each layer changes. The logic of the computer program entails the assumption that the division of flow among the layers remains constant during each time step. At the beginning of each new time step, the fraction of the total flow into each bed is recalculated.

The statements on Cards 26 through 29 establish the fraction of layer one through which the flood front passes during a given time step, thereby setting the duration of the step. The statements on Cards 57 and 77 solve Equation (3-32) for the injection rates into the various strata. The statement on Card 80 evaluates Equation (3-33) and Card 87 determines the producing water cut by Equation (3-34).

At the end of each time step the following output is given by the computer: 1) time since injection began, 2) cumulative water injected, 3) cumulative oil production, 4) oil production rate, 5) water cut, 6) unit recovery factor, and 7) the fraction of layer one which is behind the flood front.

#### Gas Storage

To solve the necessary equations for predicting the performance of stratified aquifers upon the injection of natural gas, the calcu-

lations were divided into three separate computer programs. Each of these programs was written originally in Fortran with Format for the IBM 1620. Part One calculates the basic frontal drive information. The second part makes a least squares curve fit of data from the first part; then, the third part is used to execute the remaining calculations necessary for predicting well bore pressure and radii of the two-phase flow region. The first program requires about 30 minutes execution time and the second about 3 minutes. The third program required an average of two minutes per time step on the IBM 1620. Therefore, several hours were sometimes required for a single problem. Due to difficulty in scheduling the required machine time and to the limited computer size, the third program was later revised so as to be acceptable to the IBM 1410.

A. Part One. The first program, which calculates essential frontal drive data for use in the other programs, is listed in Table IV and its flow chart is shown in Figure 13. Fortran symbols used in the gas injection programs are defined in Table V. The first program needs this input data: 1) lowest saturation at which water can flow, 2) highest water saturation at which gas can flow, 3) water viscosity, 4) gas viscosity at atmospheric pressure, 5) reservoir temperature, 6) gas gravity, 7) initial water saturation, and 8) a table of relative permeabilities to gas and water with corresponding saturations.

Gas storage reservoirs are normally operated in the pressure and temperature range where the gas deviation factor varies linearly with pressure at constant temperature. The pseudo-critical temperature and



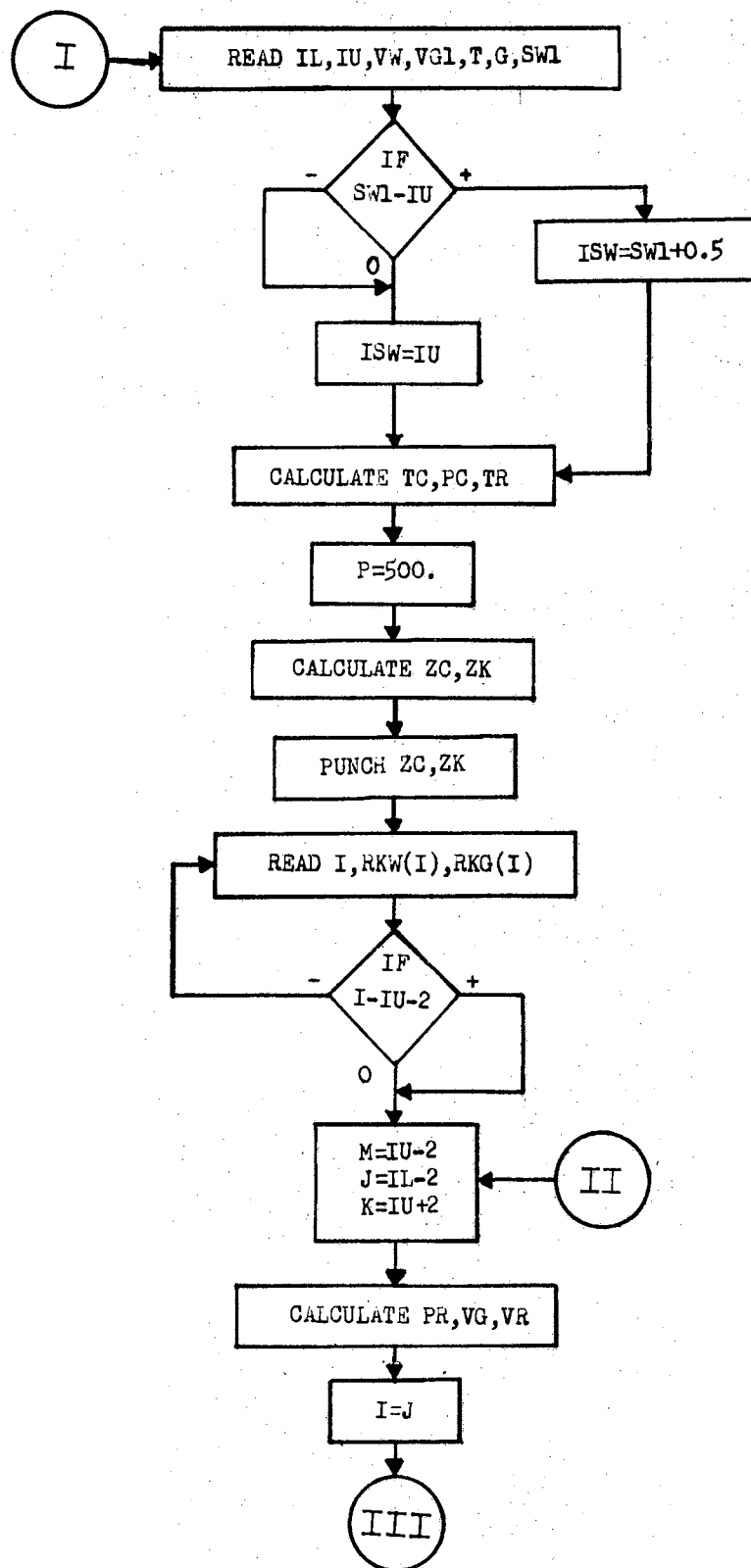


Figure 13. Flow Chart of Part One Gas Storage Program.

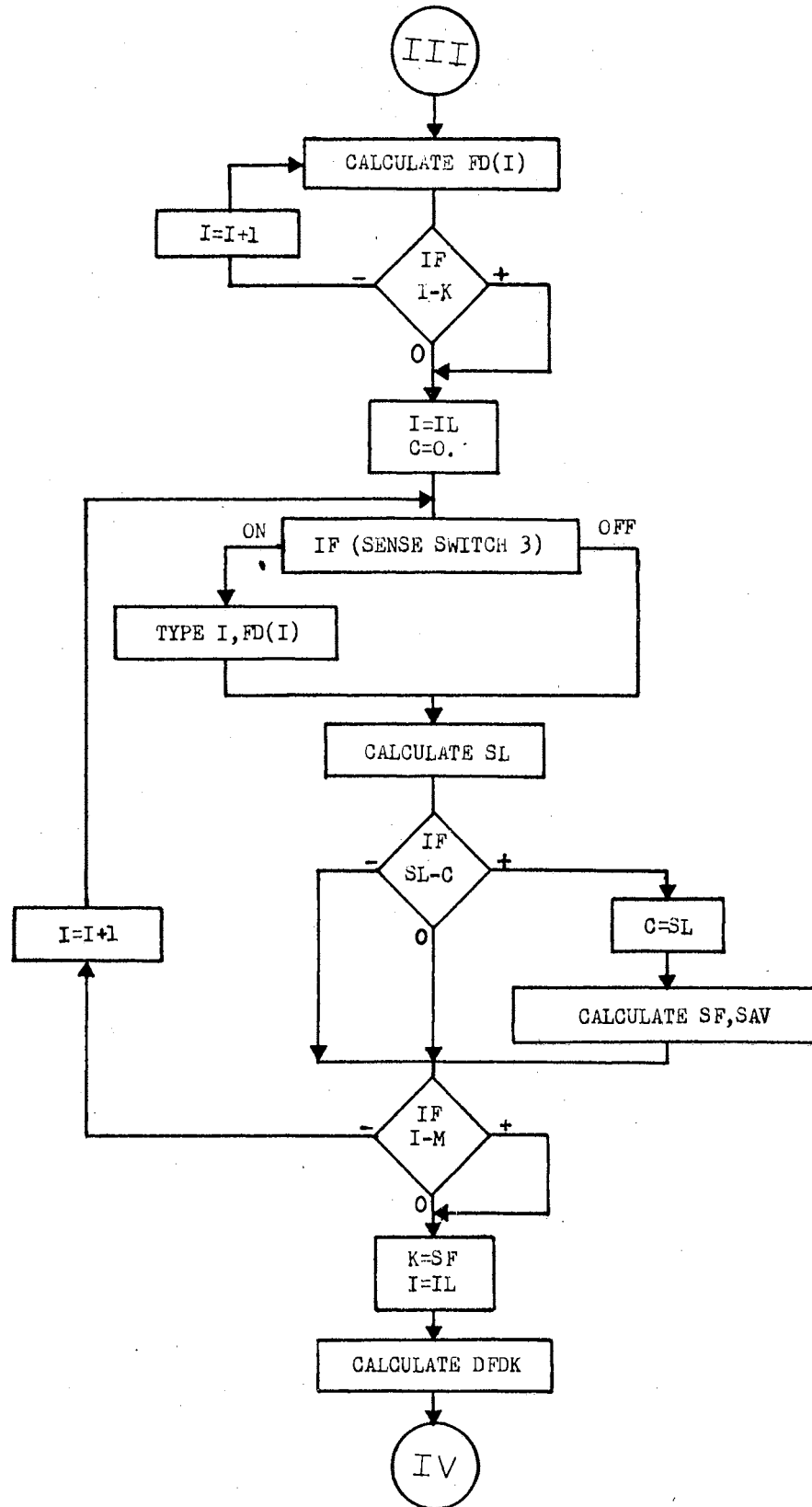


Figure 13. (Continued)

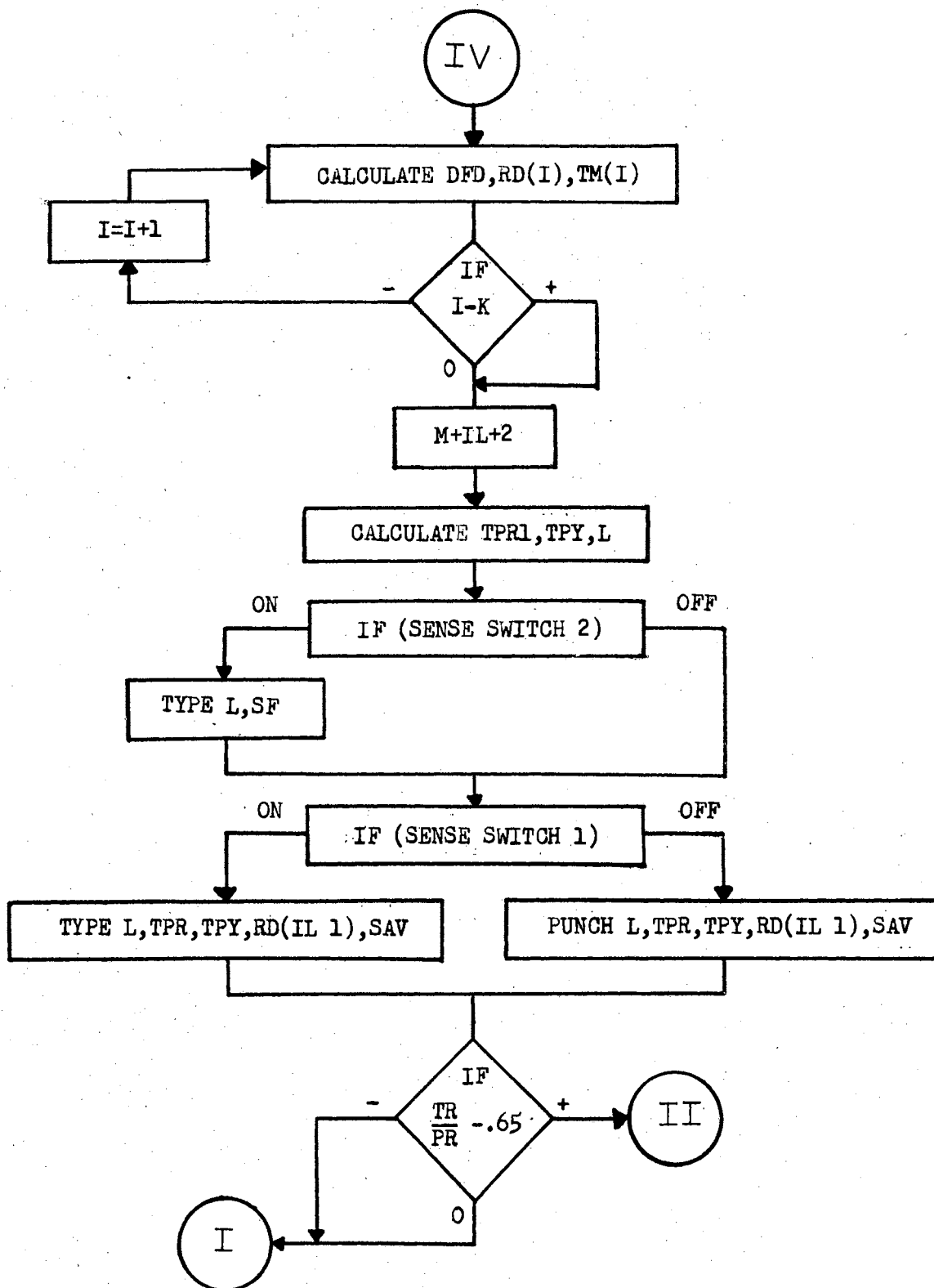


Figure 13. (Continued)



TABLE V

## FORTRAN SYMBOLS FOR GAS INJECTION PROGRAMS

A	Water saturation, percent.
AK	Average permeability of the aquifer, md.
APO	Average porosity of the aquifer, fractional.
B	Dummy variable used for programming purposes.
BK(J)	Base permeability of layer J, md.
CAP(J)	A capacity term which indicates the relative ease with which a layer accepts gas.
C	Negative slope of tangent to fractional flow curve (Program 1). Aquifer compressibility, $\text{psi}^{-1}$ (Program 3).
CI	The maximum amount which one pressure estimate can differ from the previous guess, psi.
CQD	Constant used in computing pseudo-dimensionless flow rate, $\text{psi days/ft.}^{-3}$ .
CS	A variable used in converting between reservoir and standard conditions.
CTD	Constant used in computing dimensionless time, days.
C1	Average gas saturation in the two-phase flow region less initial gas saturation.
C2	Variable used in converting between reservoir and standard conditions.
C3	Constant used in correction gas saturation outside the two-phase flow region for changes in pressure.
DFD	Derivative of fractional flow of gas with respect to saturation.
DFDK	Derivative of fractional flow at frontal saturation.
DPIC	Differential pressure across the "incompressible region", psi.
DFU	Pressure change at the interior radius of the unsteady state region, psi.
EI	Exponential integral of dimensionless time term.
FD	Fractional flow of gas.
G	Gas gravity, air = 1.
H(J)	Thickness of layer J, ft.
HA	Thickness of the aquifer, ft.
I	Water saturation in fixed point form, percent.
IL	Irreducible water saturation, percent.
IU	Highest water saturation at which gas will flow during the drainage cycle, percent.
ISW	Water saturation at the beginning of injection, percent.

TABLE V (Continued)

ITP	Number of iterations made to establish well bore pressure.
J	Fixed point variable used to identify the layers.
K	Water saturation at the front, percent (Program 1). Time step number, (Program 3).
L	Pressure increment number.
LM	Maximum value of L.
M	Used for programming purposes only.
N	Total number of layers.
P	Average pressure in the two-phase flow region, psia.
PAI	Initial pressure, psia.
PB	Base pressure for gas measurement, psia.
PC	Pseudo-critical pressure of the gas, psia.
PO(J)	Porosity of layer J, fractional.
PR	Pseudo reduced pressure of the gas.
PW	Well bore pressure, psia.
PWC	Calculate value of well bore pressure, psia.
PWP	Well bore pressure at end of previous time step, psia.
QD	Pseudo-dimensionless flow rate into the aquifer, psi.
Q(J)	Reservoir injection rate into layer J, ft <sup>3</sup> /day.
QR	Injection rate at reservoir conditions, ft <sup>3</sup> /day.
QS	Gas injection rate, SCFPD.
QT(J)	Cumulative gas stored in layer J, SCF.
R	A flow resistance factor.
RA	External radius of the steady state region and internal radius of the unsteady state region, ft.
RB(J)	Radius of the two-phase flow region in layer J, ft.
RBM(J)	Maximum previous value of RB(J), ft.
RD	Dimensionless radius.
RD1	Dimensionless radius to saturation IL + 1.
RD1S	Constant used in evaluating RD1.
RD1O	Constant used in evaluating RD1.
RKG(I)	Relative permeability to gas at saturation I, fractional.
RKW(I)	Relative permeability to water at saturation I, fractional.
RKWTG	Relative permeability to water at the gas saturation outside the two-phase flow region, fractional.
RW	Well bore radius, ft.
S	Dummy variable used in Program 2.
SAV	Average water saturation in the two-phase flow region, fractional.

TABLE V (Continued)

SAVS	Constant used in evaluating SAV.
SAVO	Constant used in evaluating SAV.
SL	Negative slope of the tangent to the fractional flow curve.
SP	Summation of pressure, psi.
SQ	Cumulative amount of gas stored in the reservoir, SCF.
SQP	SQ of the previous time step, SCF.
SWI	Water saturation at the beginning of injection, percent.
T	Reservoir temperature, °F (Program 1), °R (Program 3).
TB	Base temperature for gas measurement, °R.
TC	Pseudo-critical temperature of the gas, R.
TD	Dimensionless term involving time.
TGS	Gas saturation outside the two-phase flow region, fractional.
TI	Length of time step, days.
TIM	Time elapsed between beginning of injection and end of the previous time step, days.
TM	Total relative fluid mobility, $cp^{-1}$ .
TME	Total time elapsed since injection began, days.
TPR	Flow resistance factor for the two-phase flow region.
TPR1	Flow resistance factor for the two-phase region excluding the portion inside saturation $IL + 1$ .
TPR1B	Constant used in evaluating TPR1 from least squares curve fit.
TPR1O	Constant used in evaluating TPR1 from least squares curve fit.
TPY	Reciprocal total mobility inside $IL + 1$ , cp.
TPYS	Constant used in evaluating TPY.
TPYO	Constant used in evaluating TPY.
TR	Pseudo reduced temperature.
TT(K)	Total time elapsed between beginning of injection and end of time step K, days.
VG	Gas viscosity at reservoir conditions, cp.
VGI	Gas viscosity at reservoir temperature and atmospheric pressure, cp.
VR	Viscosity ratio.
VW	Water viscosity, cp.
X	Used for programming purposes only.
YO	Dummy variable used in Program 2.
Z	Gas deviation factor.
ZC	Constant used in evaluating Z.
ZK	Constant used in evaluating Z.
ZP	Gas deviation factor of the previous time step.

pressure of the gas are established by statements on Cards 8 and 9 which represent the correlations of Katz. (10) The statements on Cards 13, 15, and 17 determine the constants of linear variation of the gas deviation factor. The statements on Cards 28, 29, and 30 calculate fractional flow of gas at each 1% saturation interval. Statements given on Cards 33 and 34 instruct the computer to print saturation and corresponding fractional flow values when the proper console switch is turned on. The statements on Cards 35 through 40 direct calculations which are analogous to the graphical construction of a tangent to the fractional flow versus saturation curve. This procedure determines the frontal and average saturation. Dimensionless radii of the various saturations in the two-phase flow regions are calculated by using Equation (3-38) as shown by Card 47. The preceding statement evaluates the derivative of fractional flow by the method of central differences. The statement on Card 53 evaluates all except the first term of the series portion of Equation (3-39). This program, first, assumes a pressure of 500 psia then all calculations except those for the gas deviation factor are repeated at 50 psi increments until halted by the operator or until the linear approximation of gas deviation factor becomes invalid.

The gas deviation factor constants are the first output data punched. Then, for each pressure increment the following data are given: 1) pressure increment number, 2) value of the series portion of Equation (3-39) excluding the first term, 3) reciprocal relative mobility in the cylindrical shell nearest the well bore, 4) dimensionless radius of water saturation 1% greater than that of the well bore, and 5) average water saturation of the two-phase flow region.

B. Part Two. Plots of each of the output quantities from the first part gave very nearly linear variation with pressure. Due to this fortunate circumstance, a short program utilizing the method of least squares was written to determine the equation of the best straight line fit for each of the quantities.

The input to the second program is the number of pressure increments and all the punched output from the first part except the first card. The output of the second program is in the form of a slope and zero pressure intercept of the straight line equations for: 1) the series portion Equation (3-39) except for the first term, 2) reciprocal relative mobility within 1% saturation of the well bore, 3) dimensionless radius to 1% saturation away from the well bore, and 4) average water saturation in the two-phase flow zone. A flow chart of the second program is shown in Figure 14. Table VI is its Fortran listing.

C. Part Three. The purpose of the third program is to apply data from the first and second programs to a stratified system of the type represented by Figure 9 in such a manner as to predict well bore pressure and radii of the two-phase flow regions. Table VII is the program listing and Figure 15 is its flow chart. Symbols for this program are also defined in Table V.

Input data required for the third program includes: 1) well bore radius, 2) radius of the "incompressible core", 3) aquifer permeability, 4) aquifer porosity, 5) aquifer thickness, 6) initial aquifer pressure, 7) amount of gas initially in place, 8) base pressure for gas measurement, 9) base temperature for gas measurement, 10) reservoir temperature, 11) water viscosity, 12) gas saturation in any immobile gas regions, 13)

TABLE VI

## CURVE FIT FOR FRONTAL DRIVE DATA

C	GAS STORAGE IN A STRATIFIED RADIAL RESERVOIR, PART 2	001
C	CURVE-FITTING FRONTAL DRIVE DATA FOR INJECTION	002
C	USE ALL PUNCHED OUTPUT FROM PART 1, EXCEPT FIRSTCARD	003
	DIMENSION TPR1(25),TPY(25),RD1(25),SAV(25),Y(25)	004
10	READ 3,LM	5
	DO 30 L=1,LM	6
30	READ 1,L,TPR1(L),TPY(L),RD1(L),SAV(L)	007
	AL=LM	8
	K=-1	9
12	IF (K)14,15,13	010
13	IF (K-2)16,17,10	011
14	DO 20 L=1,LM	012
20	Y(L)=TPR1(L)	013
	GO TO 18	014
15	DO 21 L=1,LM	015
21	Y(L)=TPY(L)	016
	GO TO 18	017
16	DO 22 L=1,LM	018
22	Y(L)=RD1(L)	019
	GO TO 18	020
17	DO 23 L=1,LM	021
23	Y(L)=SAV(L)	022
18	P=500.	023
	SP=0.	024
	SY=0.	025
	SPY=0.	026
	SP2=0.	027
	DO 19 L=1,LM	028
	SP=SP+P	029
	SY=SY+Y(L)	030
	SPY=SPY+(P*Y(L))	031
	SP2=SP2+(P**2)	032
19	P=P+50.	033
	Y0=((SY*SP2)-(SPY*SP))/((AL*SP2)-(SP**2))	034
	S=((AL*SPY)-(SP*SY))/((AL*SP2)-(SP**2))	035
	PUNCH 2,S,Y0	036
	K=K+1	037
	GO TO 12	038
1	FORMAT (I3,E17.0,E17.0,E17.0,F12.8)	039
2	FORMAT (E17.8,E17.8)	040
3	FORMAT (I5)	041
	END	042

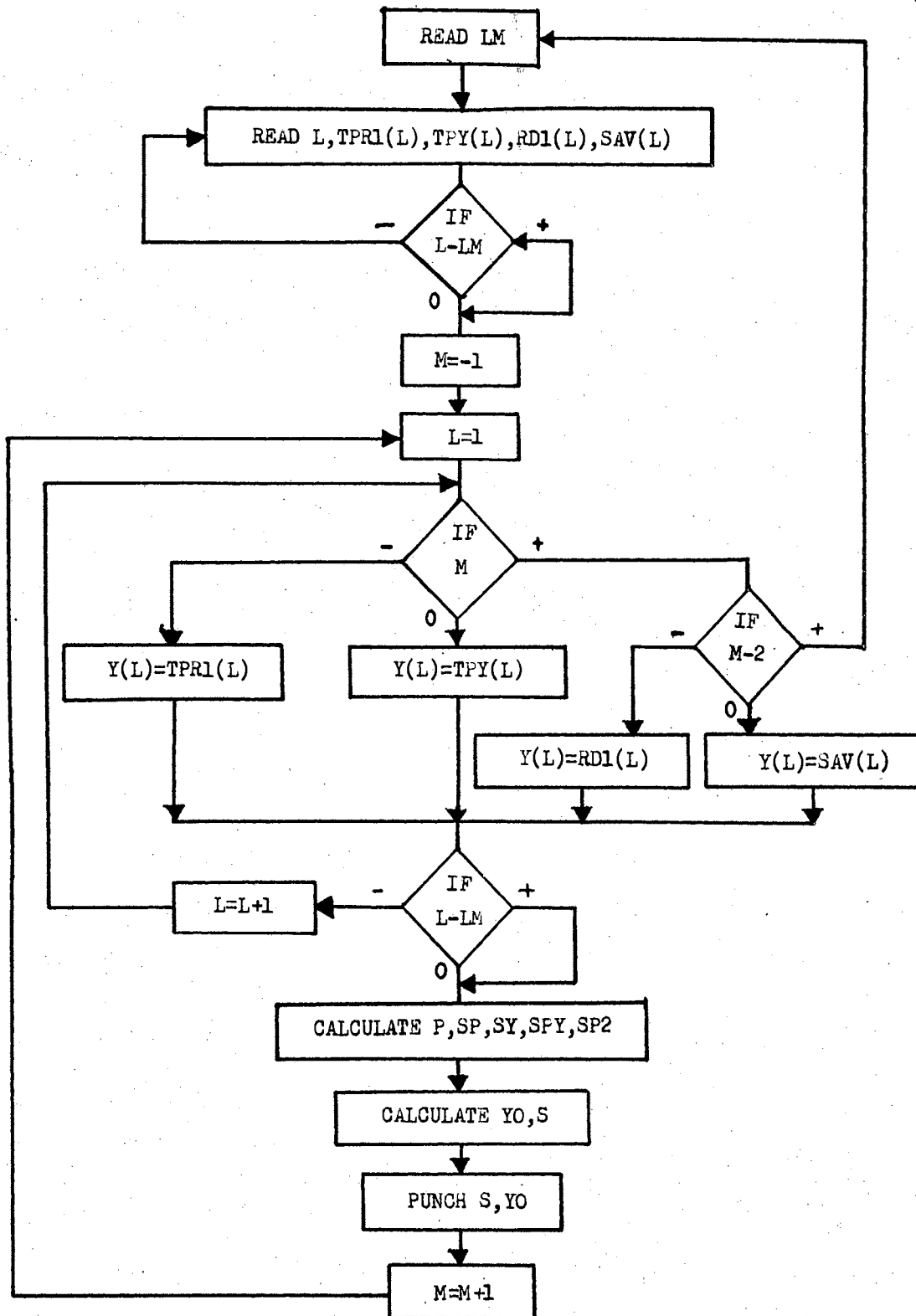


Figure 14. Flow Chart of Part Two Gas Storage Program.

TABLE VII

## GAS INJECTION PERFORMANCE PREDICTIONS

C	GAS STORAGE IN A STRATIFIED RADIAL RESERVOIR	000
C	PART 3 PRESSURE AND RADIUS, ASSUMING A COMMON ACQUIFER	001
C	INPUT TEMPERATURES AND PRESSURES MUST BE ABSOLUTE	002
	DIMENSION QD(200),TT(200)	003
	DIMENSION H(9),BK(9),PO(9),Q(9),QT(9),RB(9),RBM(9),CAP(9)	004
	READ 9	5
	PUNCH 9	6
	READ 1,RW,RA,AK,AP0,HA,PAI, SQP	007
	READ 2,PB,TB,T,VW,TGS,RKWTG,C,N	008
	READ 3,TPR1S,TPR10	9
	READ 3,TPYS,TPY0	010
	READ 3,RD1S,RD10	011
	READ 3,SAVS,SAVO	012
	J = 0	013
10	J = J + 1	014
	READ 5,J,H(J),BK(J),PO(J),RBM(J),RB(J),QT(J)	015
	IF (J-N)10,11,11	016
11	PWP=PAI	017
	PW=PAI	018
	CS=PB*T/TB	019
	TIM=0.	020
	CQD=(-.1257878E-04)*VW/(AK*HA)	021
	CTD=39.505*(RA**2)*VW*C/AK	022
	READ 3,ZC,ZK	023
12	READ 4,K,QS,TME	024
	TT(K)=TME	025
	TI=TME-TIM	026
	TIM=TME	027
	ITP=0	028
	CI=10.	029
	SQ=SQP+(QS*TI)	030
13	Z=ZC-(ZK*PW)	031
	TPR1=TPR10+(TPR1S*PW)	032
	TPY=TPY0+(TPYS*PW)	033
	RD1=RD10+(RD1S*PW)	034
	SAV=SAVO+(SAVS*PW)	035
	SC=0.	036
	J=0	037
101	J=J+1	038
	IF ((RB(J)*RD1)-RW)33,33,34	039
33	TPR=TPR1	040
	GO TO 66	041
34	TPR=TPR1+(TPY*LOGF(RD1*RB(J)/RW))	042
66	R=(VW*((LOGF(RA/RBM(J)))+(LOGF(RBM(J)/RB(J))/RKWTG))+TPR)	043
	CAP(J)=H(J)*BK(J)/R	044
	SC=SC+CAP(J)	045
	IF (J-N)101,29,29	046
29	IF (ITP)41,41,40	047
41	ZP=Z	048
	GO TO 77	049
40	IF (K-1)77,77,80	050
80	DPU=DPU-(EI*(QD(K)-QD(K-1)))	051
77	QR=((SQ*Z/PW)-(SQP*ZP/PWP))*CS/TI	052
	IF (QR)67,78,78	053
67	QR=Q.	054
78	QD(K)=CQD*QR	055
	IF (ITP)76,76,75	056
75	IF (K-1)76,76,81	057
81	DPU=DPU+(EI*(QD(K)-QD(K-1)))	058
	GO TO 28	059
76	M=0	060
102	M=M+1	061
	IF (M-1)18,18,19	062
18	TD=CTD/TME	063
	GO TO 17	064



TABLE VII (Continued)

19	TD=CTD/(TME-TT(M-1))	065
17	EI=.5772157+LOGF(TD)-TD+((TD**2)/4.)-((TD**3)/18.)+((TD**4)/96.)	066
	IF (M-1)20,20,21	067
20	DPU=EI*QD(1)	068
	GO TO 74	069
21	DPU=DPU+(EI*(QD(M)-QD(M-1)))	070
74	IF (M-K)102,28,28	071
28	IF (K-1)72,72,30	072
72	IF (ITP)73,73,30	073
73	C3=TGS*PW/Z	074
	PUNCH 7	075
	PUNCH 8	076
30	J=0	77
39	J=J+1	078
	Q(J)=QR*CAP(J)/SC	079
	IF (J-N)39,103,103	080
103	DPIC=25.11*Q(1)/CAP(1)	081
	PWC=PAI+DPU+DPIC	082
	IF (ABS(PW-PWC)-1.)55,55,53	083
53	ITP=ITP+1	084
	IF (ITP-10)50,50,90	085
90	IF (CI-.5)55,55,79	086
79	CI=CI-.5	087
50	IF (PW-PWC+CI)57,59,56	088
56	IF (PWC-PW+CI)58,59,59	089
57	PW=PW+CI	090
	GO TO 13	091
58	PW=PW-CI	092
	GO TO 13	093
59	PW=PWC	094
	GO TO 40	095
55	PWP=PW	096
	SQP=SQ	097
	TGS=C3*Z/PW	098
	C1=1.-SAV-TGS	099
	C2=PW/(Z*CS)	100
	SQT=0.	101
	J=0	102
22	J=J+1	103
	QT(J)=QT(J)+(Q(J)*C2*TI)	104
	SQT=SQT+QT(J)	105
	IF (J-N)22,104,104	106
104	SQT=SQ/SQT	107
	J=1	108
26	QT(J)=QT(J)*SQT	109
	B=RB(J)	110
	IF (B-RBM(J))105,106,106	111
105	RB(J)=SQRTF(((QT(J)/(C2*3.1416*H(J)*PO(J)))-((RBM(J)**2)*TGS))/C1)	112
	IF (RB(J)-RBM(J))88,88,106	113
106	RB(J)=SQRTF(QT(J)/(C2*3.14159*H(J)*PO(J)*(1.-SAV)))	114
88	IF (RB(J)-B)89,91,91	115
89	RB(J)=B	116
91	IF (RB(J)-RBM(J))62,62,61	117
61	RBM(J)=RB(J)	118
62	PUNCH 6,K,J,RB(J),QT(J),SQ,PW,TME	119
	J=J+1	120
	IF (J-N)26,26,12	121
1	FORMAT (F4.3,F8.0,F7.0,F7.3,F7.1,F7.0,E16.0)	122
2	FORMAT (F6.3,F7.0,F7.0,F7.3,F7.3,F7.3,E16.0,I6)	123
3	FORMAT (E17.0,E17.0)	124
4	FORMAT (I5,F15.0,F8.0)	125
5	FORMAT (I2,F6.0,F7.0,F7.3,F7.0,F7.0,E16.0)	126
6	FORMAT (1H ,I3,I5,F9.0,E17.8,E17.8,F11.1,F9.2)	127
7	FORMAT (17H ID J RB(J),9X,5HQ(T(J)),13X,2HSQ,13X,2HPW,7X,3HTME)	128
8	FORMAT (5X,10HLAYER FT,12X,3HSCF,14X,3HSCF,11X,4HPSIA,5X,4HDAYS)	129
9	FORMAT (49H IDENTIFICATION )	130
	END	131

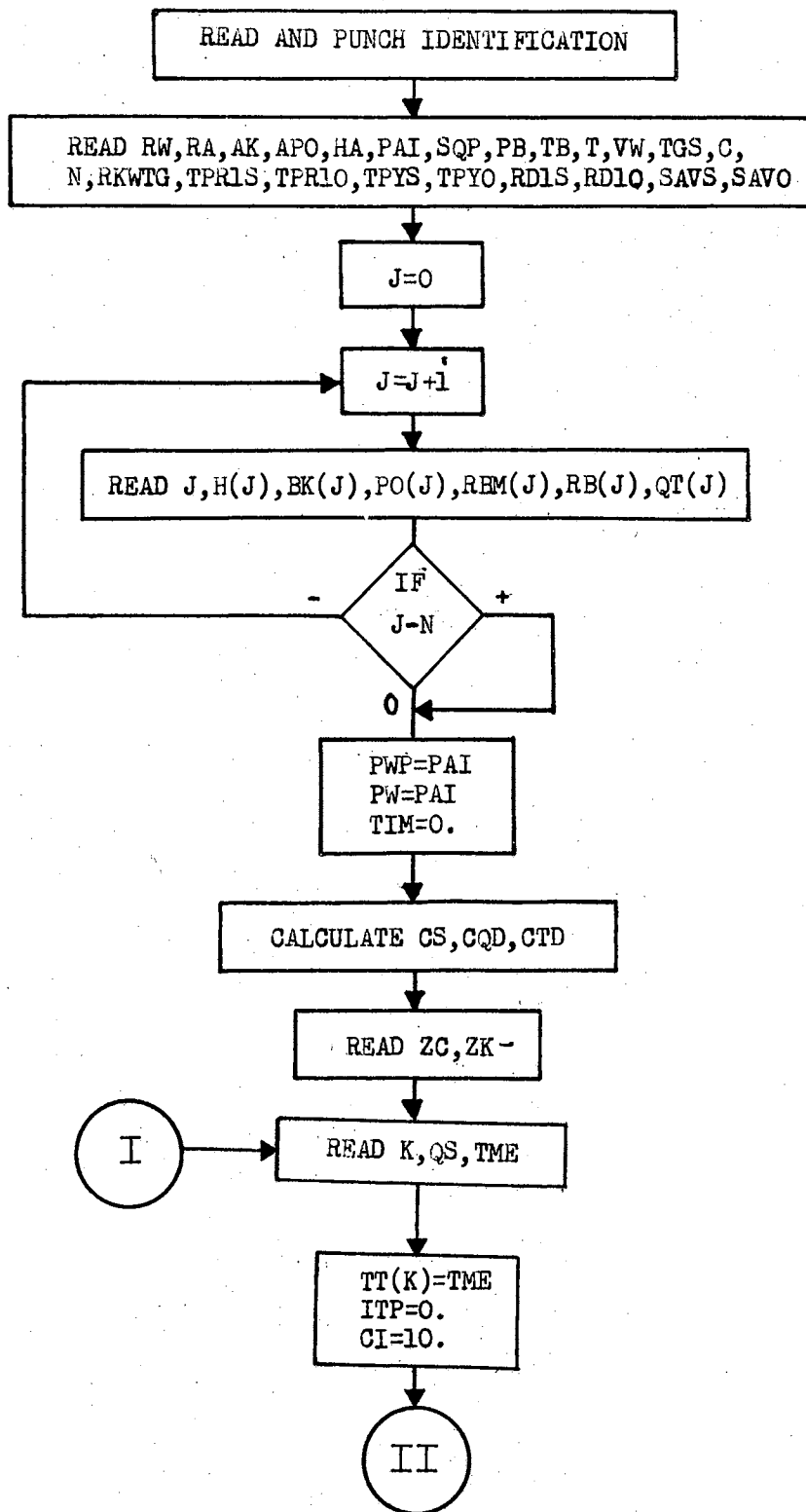


Figure 15. Flow Chart of Part Three Gas Storage Program.

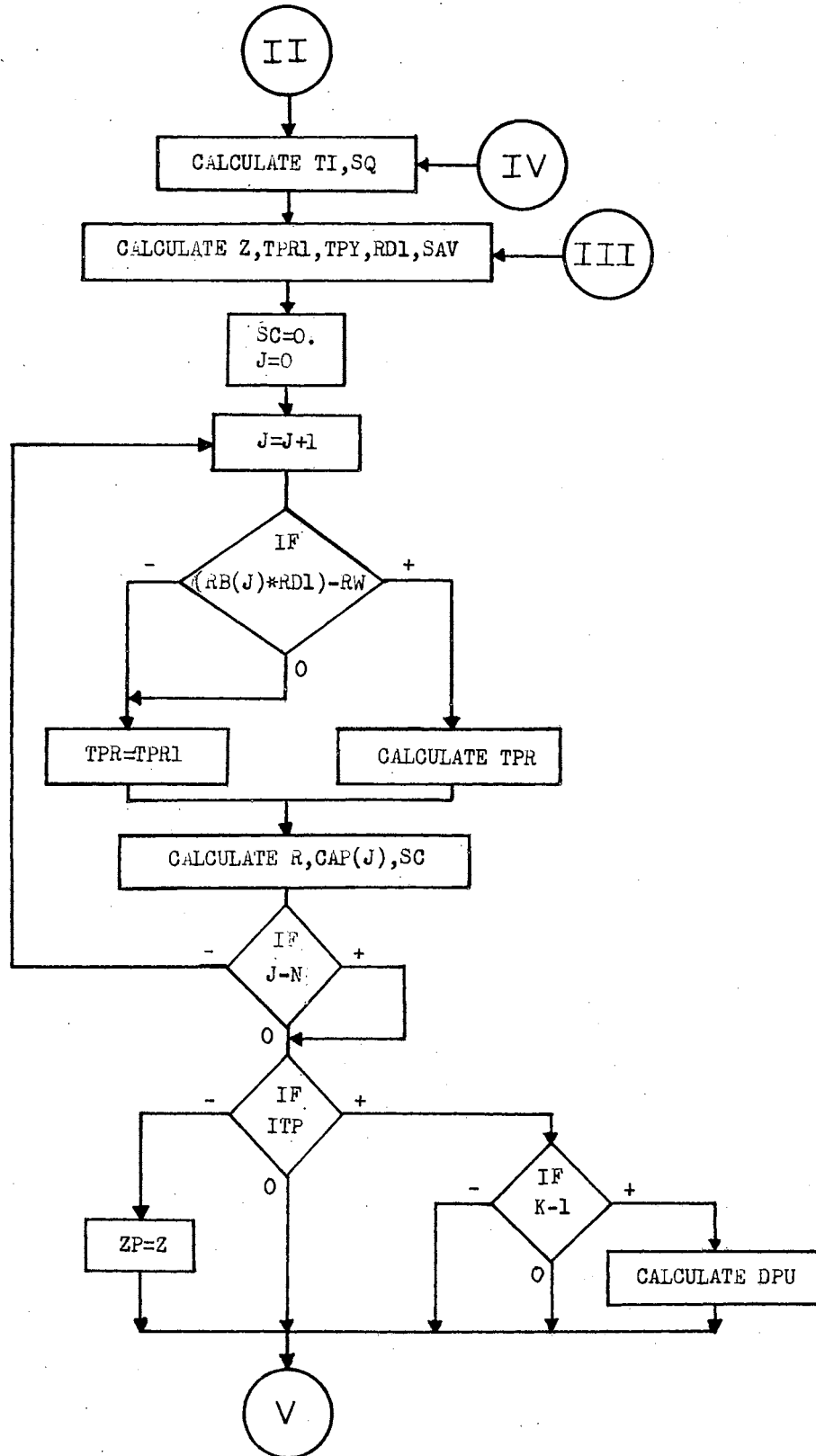


Figure 15. (Continued)

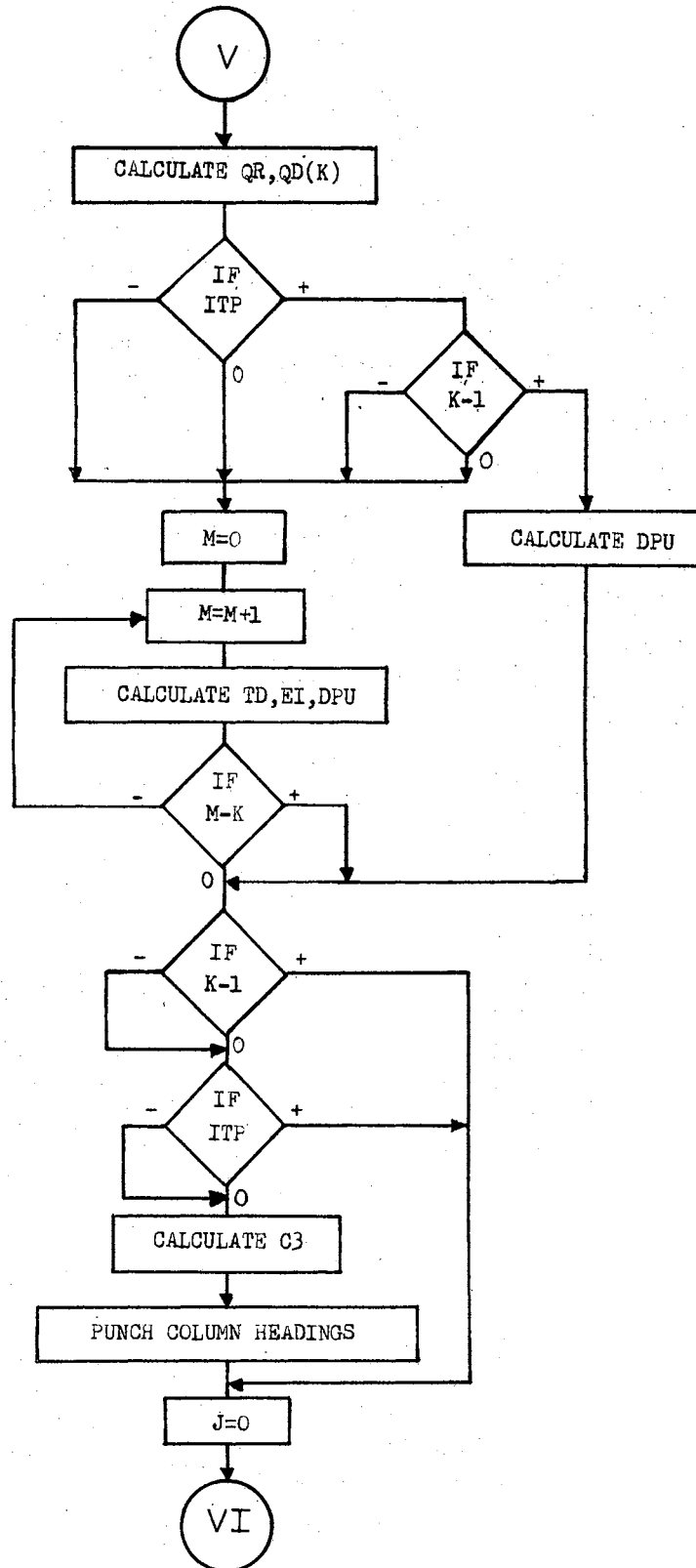


Figure 15. (Continued)

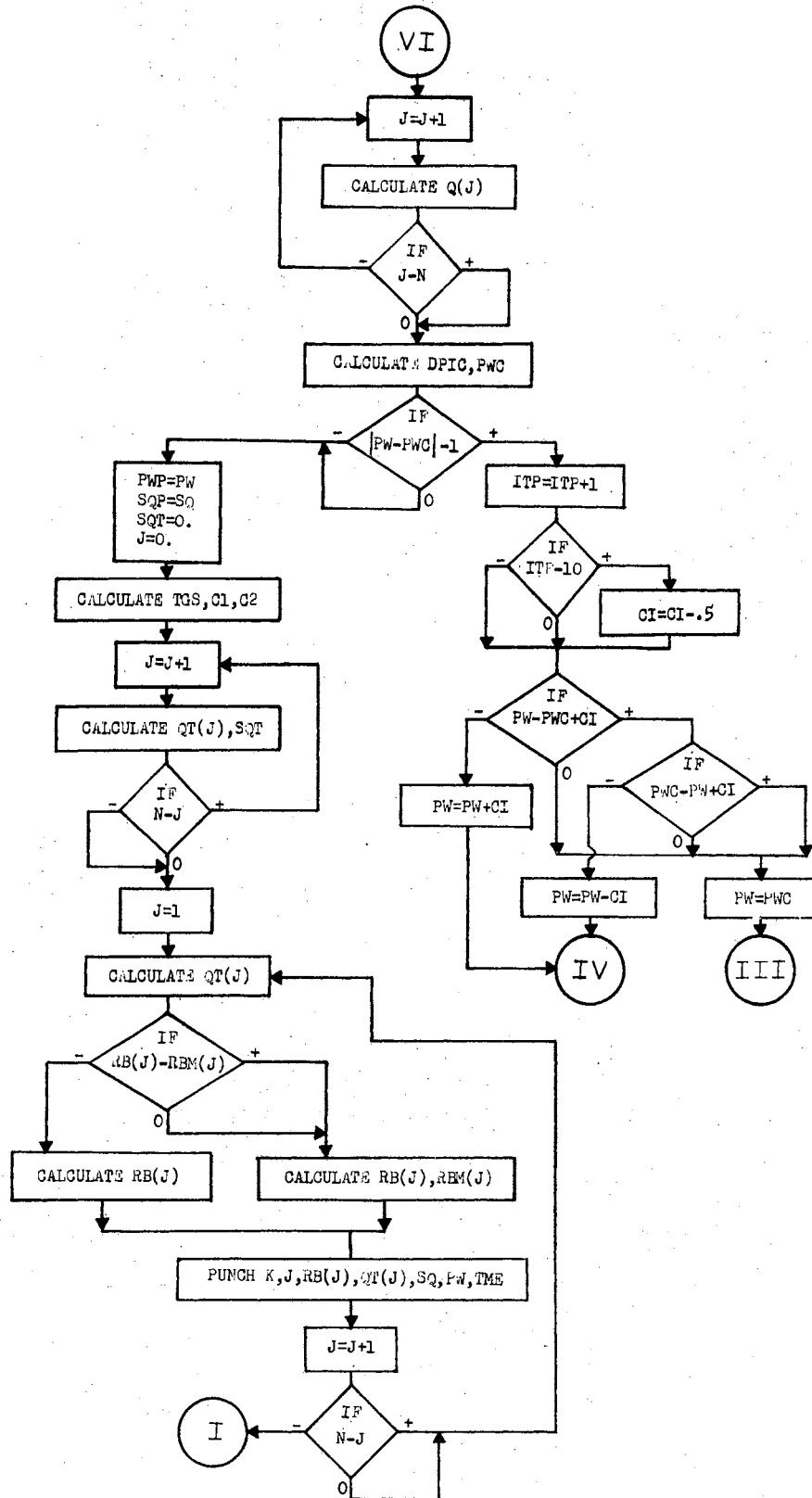


Figure 15. (Continued)

relative permeability to water of any immobile gas regions, 14) aquifer compressibility, 15) number of layers, 16) all the output data from the second program, 17) gas deviation factor constants from the first program, and 18) a table of injection rates and corresponding times. For each layer this additional data is needed: 1) layer number, 2) thickness, 3) absolute permeability, 4) porosity, 5) maximum previous radius of the two-phase flow region, 6) current radius of the two-phase flow region, and 7) cumulative gas in the layer.

This program first assumes a value of well bore pressure then calculates a reservoir flow rate, divides the flow among the layers, evaluates the unsteady state pressure change, then calculates a value for the well bore pressure. If the estimated and calculated values of well bore pressure do not agree to within one psi, a new pressure is estimated and the calculations are repeated until agreement is reached. New radii of the two-phase flow regions are then calculated. The whole process is repeated for each time step. It was found that if the estimate of well bore pressure is allowed to change too much between iterations, an extraneous value of pressure will be converged upon occasionally. To prevent this, a new pressure estimate is not allowed vary more than 10 psi from the previous estimate. Statements on Cards 29 and 85 through 95 establish the pressure estimates.

The gas deviation factor and two-phase flow quantities from the previous programs are evaluated by instructions on Cards 31 through 35. The average reservoir flow rate for a time step is defined on Card 52 as the change in volume of gas in the reservoir divided by the duration of the time step. Pseudo-dimensionless flow rates, Equation (3-44), are

determined by Cards 21 and 55. Dimensionless time is evaluated by statements on Cards 22, 63, and 65. Upon comparison with Equation (3-43), it is noted that a minus sign has been omitted in the calculation of dimensionless time. The sign was omitted due to the method used to evaluate the exponential integral.

The exponential integral is defined as

$$Ei(X) = \int_X^{\infty} \frac{e^{-x} dx}{x} \quad (4-1)$$

It has been shown that the exponential integral may be evaluated by the following series

$$Ei(-X) = 0.57722 + \ln X - X + \frac{X^2}{2 \cdot 2!} - \frac{X^3}{3 \cdot 3!} + \dots \pm \frac{X^n}{n \cdot n!} \quad (4-2)$$

Equation (3-45) is evaluated to give the unsteady state pressure change at the exterior radius of the "incompressible core" by the statements of Cards 68 and 70. A flow resistivity factor is calculated for each layer, Equation (3-50), by statements on Cards 39-43. The summation for Equation (3-49) is made by Cards 44 and 45. The actual division of flow is made by the statements of Card 79. The radii of the two-phase flow zones are calculated by statements on either Card 112 or Card 114.

At the end of each time step this output is punched for each layer: 1) time step number, 2) layer number, 3) radius of two-phase flow, 4) total amount of gas in that layer, 5) total amount of gas in all layers, 6) well bore pressure, and 7) time since injection began.

## CHAPTER V

### EXAMPLE PROBLEMS AND RESULTS

An example water flood problem was solved by the methods presented by Stiles and by Dykstra and Parsons for comparison with results of the frontal drive method. All the necessary data for any of the three techniques is listed in Table VIII. It should be noted that not all the given information is required for each of the techniques.

A plot of oil production rates versus time is shown in Figure 16. It is noted that the peak production rate given by the frontal drive method is much lower than that predicted by the other two techniques. The predicted high early production rates are chief criticisms of results of the Stiles and Dykstra-Parsons calculations. A comparison with published water flood performances by Gurrero and Earlougher (8) indicates that the peak production rate given by the frontal drive technique is more realistic than those of the other methods. During the later part of the life of the water flood the frontal drive method indicates slightly higher production rates than the other methods. It is noted that some points given by the frontal drive calculations do not fall on a smooth decline curve. This is explained by the fact that the reservoir was divided into only 10 layers for the frontal drive programs while 29 layers were used for the other methods. As expected, Figure 17 shows a less optimistic prediction of cumulative oil recovery



TABLE VIII  
 DATA FOR WATER FLOOD EXAMPLE

VO	VW	BO	WIR	CW	SG	BV	SE	E	CUT	IL	IU
4.34	0.82	1.073	100.	24.	17.	100.	.85	1.0	.98	24	78
I	RKO	RKW			I	RKO	RKW				
22	.80	.00			23	.80	.00				
24	.80	.00			25	.791	.001				
26	.781	.002			27	.770	.004				
28	.757	.006			29	.744	.008				
30	.727	.0105			31	.710	.013				
32	.692	.015			33	.672	.018				
34	.649	.012			35	.624	.024				
36	.597	.027			37	.564	.030				
38	.529	.033			39	.490	.036				
40	.457	.040			41	.428	.043				
42	.402	.047			43	.377	.051				
44	.354	.055			45	.332	.058				
46	.311	.062			47	.292	.066				
48	.274	.071			49	.256	.075				
50	.240	.080			51	.224	.085				
52	.208	.090			53	.193	.095				
54	.178	.100			55	.164	.105				
56	.150	.111			57	.138	.117				
58	.126	.124			59	.116	.130				
60	.102	.135			61	.091	.144				
62	.081	.146			63	.072	.151				
64	.064	.155			65	.056	.160				
66	.048	.165			67	.041	.169				
68	.035	.173			69	.030	.177				
70	.025	.181			71	.020	.184				
72	.016	.187			73	.012	.190				
74	.009	.193			75	.006	.195				
76	.0035	.197			77	.001	.199				
78	.000	.200			79	.000	.200				
80	.000	.200									

STRATIFICATION DATA  
 USED IN FRONTAL DRIVE PROGRAMS

J	H(J)	BK(J)
1	5.0	39.0
2	4.0	61.3
3	4.0	84.7
4	3.0	128.0
5	4.0	171.3
6	1.0	228.0
7	4.0	278.0
8	2.0	328.5
9	1.0	454.0
10	1.0	776.0

STRATIFICATION DATA  
 USED WITH OTHER METHODS

J	H(J)	BK(J)
1	1.0	776.
2	1.0	454.
3	1.0	349.
4	1.0	308.
5	1.0	295.
6	1.0	282.
7	1.0	273.
8	1.0	262.
9	1.0	228.
10	1.0	187.
11	1.0	178.
12	1.0	161.
13	1.0	159.
14	1.0	148.
15	1.0	127.
16	1.0	109.
17	1.0	88.
18	1.0	87.
19	1.0	87.
20	1.0	77.
21	1.0	71.
22	1.0	62.
23	1.0	58.
24	1.0	54.
25	1.0	50.
26	1.0	47.
27	1.0	47.
28	1.0	35.
29	1.0	16.

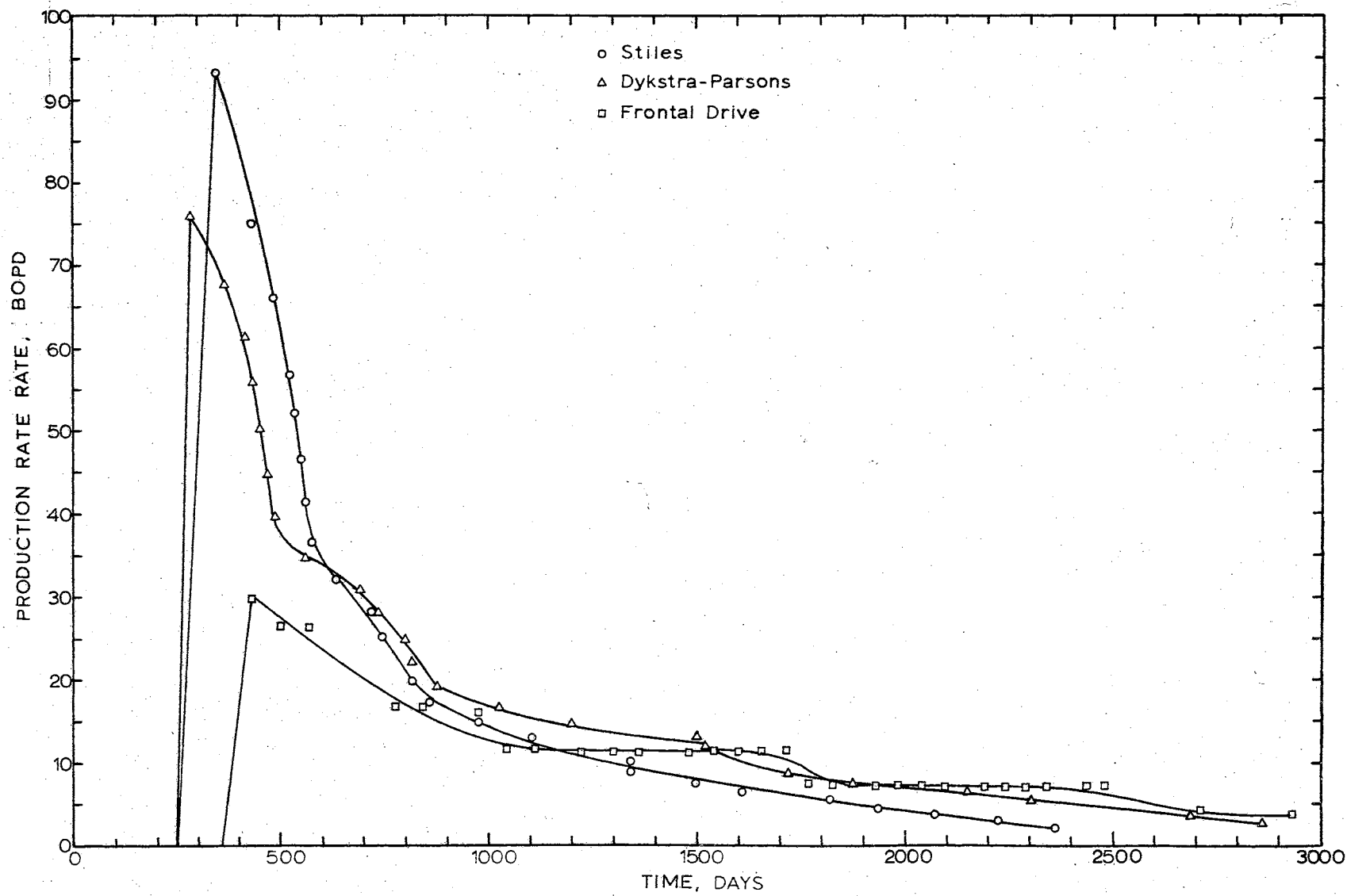


Figure 16. Comparison of Oil Production Rate Predictions.

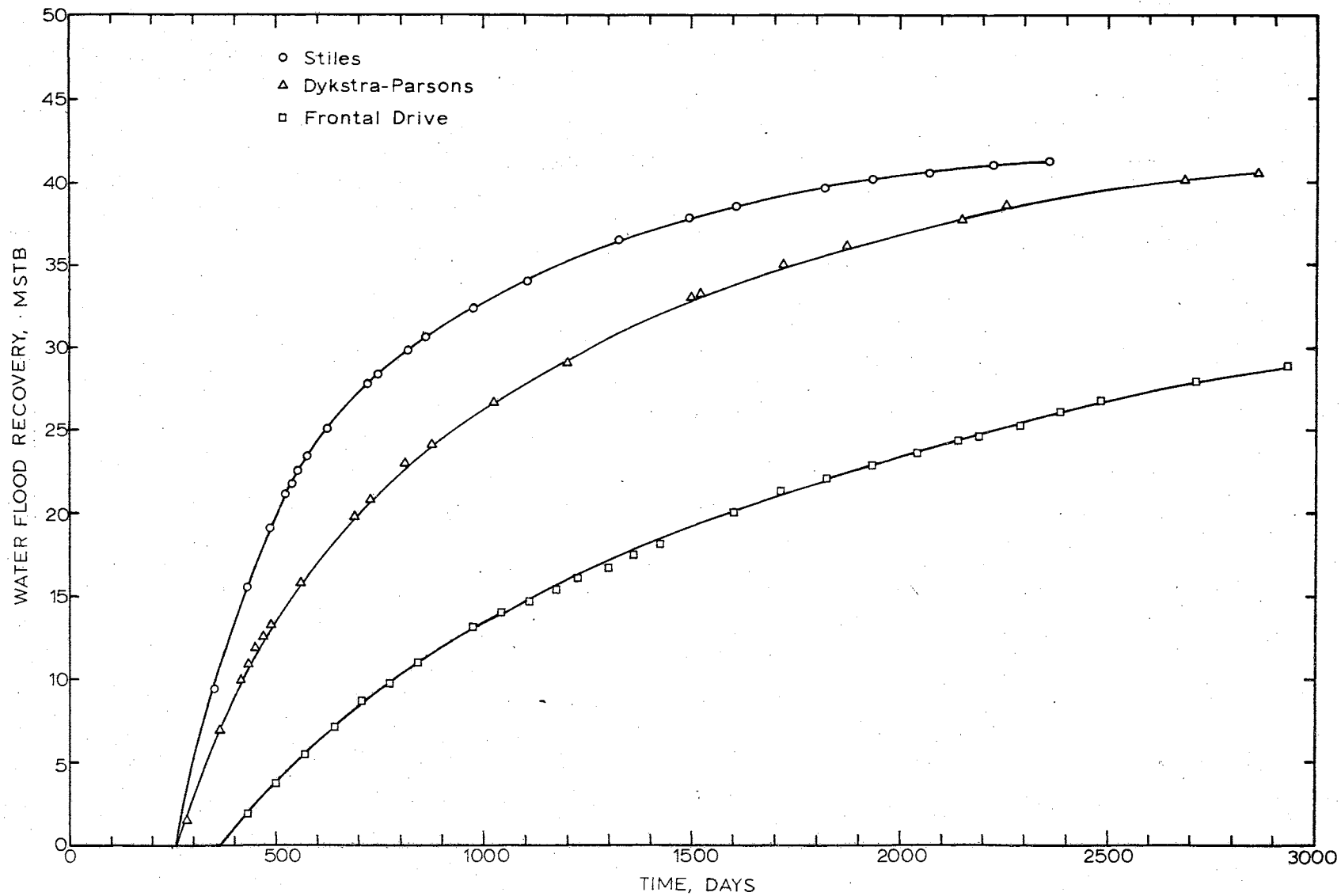


Figure 17. Comparison of Oil Recovery Predictions.

by the frontal drive technique than by the other approaches.

Two example problems of gas injection into a stratified reservoir were solved by the computer programs of the previous chapter. The two cases were identical except that in the first, Case I, no gas was initially in the reservoir while the second, Case II, assumed an immobile gas saturation existed within definite radii. Both examples were for a three layer reservoir.

Tables IX and X show computer input data for the case with no initial gas present. The input data includes the output data from the first two programs. The output data from the third program is shown in Table XI.

Figure 18 shows injection rate, well bore pressure, and radii of the two-phase flow regions for Case I as functions of time. It is noted that upon initiation of injection the well bore pressure almost instantly leaped from 1100 psia to more than 1400 psia then began to decline even though a constant injection rate was maintained. If unsteady state single-phase flow had existed, the pressure would have continuously increased at constant injection rate. The decreasing rather than increasing pressure shows the effect of the two-phase flow regions being formed around the well bore. After seven days, gas injection was halted; but, the radius of the two-phase flow region in each layer continued to grow as the unsteady state pressure build-up decayed and allowed gas expansion. After 12 days, injection was resumed at twice the former rate but the pressure increase was much more gradual than during the first injection. This was due to the existence of the two-phase flow regions.

TABLE IX

## TWO-PHASE FLOW DATA, CASE I

## PART ONE INPUT DATA

IL	IU	VW	VG1	T	G	SW1
25	94	.874	.0106	79.	.66	100.
I	RKW	RKG	I	RKW	RKG	
23	.0000	.5340	24	.0000	.5180	
25	.0000	.5020	26	.0002	.4840	
27	.0005	.4680	28	.0007	.4540	
29	.0010	.4375	30	.0012	.4230	
31	.0015	.4060	32	.0017	.3910	
33	.0020	.3760	34	.0022	.3620	
35	.0025	.3475	36	.0027	.3330	
37	.0030	.3190	38	.0032	.3050	
39	.0035	.2910	40	.0037	.2765	
41	.0040	.2630	42	.0042	.2500	
43	.0045	.2370	44	.0047	.2240	
45	.0050	.2110	46	.0055	.1980	
47	.0060	.1880	48	.0065	.1770	
49	.0075	.1625	50	.0090	.1510	
51	.0120	.1410	52	.0150	.1300	
53	.0180	.1200	54	.0220	.1090	
55	.0250	.1000	56	.0290	.0905	
57	.0335	.0830	58	.0380	.0745	
59	.0445	.0665	60	.0500	.0582	
61	.0580	.0510	62	.0635	.0440	
63	.0730	.0380	64	.0815	.0320	
65	.0900	.0280	66	.1000	.0240	
67	.1110	.0208	68	.1210	.0180	
69	.1340	.0160	70	.1470	.0145	
71	.1620	.0130	72	.1800	.0120	
73	.2000	.0110	74	.2170	.0105	
75	.2320	.0100	76	.2470	.0096	
77	.2690	.0090	78	.2910	.0082	
79	.3090	.0077	80	.3570	.0074	
81	.3940	.0070	82	.4230	.0065	
83	.4690	.0060	84	.5130	.0054	
85	.5650	.0049	86	.6200	.0044	
87	.6630	.0038	88	.7130	.0033	
89	.7550	.0028	90	.8000	.0024	
91	.830	.0019	92	.8900	.0012	
93	.9350	.0005	94	.9800	.0000	
95	.9800	.0000	96	.9800	.0000	

## PART TWO INPUT DATA

LM  
15

L	TPR1(L)	TPY(L)	RD1(L)	SAV(L)	
1	.75404497E 00	.19984386E-01	.14159553E-01	.69500210	Z002
2	.76550473E 00	.20466309E-01	.14275824E-01	.69271120	Z003
3	.77610525E 00	.20916412E-01	.14326407E-01	.69057160	Z004
4	.78578815E 00	.21339203E-01	.14449799E-01	.68856180	Z005
5	.79486365E 00	.21738262E-01	.14515982E-01	.68666480	Z006
6	.80324138E 00	.22116482E-01	.14643296E-01	.68486690	Z007
7	.81117795E 00	.22476236E-01	.14713827E-01	.68315680	Z008
8	.81864662E 00	.22819504E-01	.14786187E-01	.68152500	Z009
9	.81756384E 00	.23147945E-01	.14961765E-01	.68023930	Z010
10	.82506067E 00	.23462971E-01	.15031538E-01	.67901770	Z011
11	.83221175E 00	.23765799E-01	.15094719E-01	.67784340	Z012
12	.83913788E 00	.24057473E-01	.15095799E-01	.67671240	Z013
13	.84564928E 00	.24338912E-01	.15169876E-01	.67562100	Z014
14	.85188568E 00	.24610912E-01	.15244762E-01	.67456630	Z015
15	.85798734E 00	.24874183E-01	.15250643E-01	.67354540	Z016

TABLE X

## TWO-PHASE, STRATIFICATION AND INJECTION; CASE I

## INITIAL INJECTION NO GAS IN PLACE 3 LAYERS

RW	RA	AK	APO	HA	PAI	SQP	
.250	1758.	500.	.170	58.0	1100.	.00000000E-00	
RB	TB	T	VW	TGS	RKWTG	C	N
14.730	520.	539.	.874	.250	.168	.60000000E-05	3

## PART TWO OUTPUT DATA

.14064857E-03	.69237238E-00
.68949142E-05	.16813647E-01
.16438190E-05	.13384085E-01
-.30163809E-04	.70834666E-00

J	H(J)	BK(J)	PO(J)	RBM(J)	RB(J)	QT(J)
1	20.0	60.	.154	.250	.250	.00000000E-00
2	8.0	400.	.175	.250	.250	.00000000E-00
3	4.5	560.	.180	.250	.250	.00000000E-00

ZC	ZK
.98237980E 00	.14360596E-03

K	QS	TME
1	2000000.	.0100
2	2000000.	.0300
3	2000000.	.0600
4	2000000.	.1000
5	2000000.	.1800
6	2000000.	.2700
7	2000000.	.4400
8	2000000.	.6500
9	2000000.	.8500
10	2000000.	1.500
11	2000000.	3.0
12	2000000.	5.0
13	2000000.	7.0
14	0000000.	8.0
15	0000000.	10.0
16	0000000.	12.0
17	4000000.	13.0
18	4000000.	15.0
19	4000000.	17.0
20	4000000.	19.0
21	3000000.	20.0
22	3000000.	22.0
23	3000000.	25.0
24	0000000.	26.0
25	0000000.	30.0
26	5000000.	31.0
27	5000000.	33.0
28	5000000.	35.0
29	5000000.	37.0
30	3000000.	38.0

TABLE XI  
RESERVOIR PERFORMANCE, CASE I

INITIAL ID	INJECTION J	NO GAS RB(J) IN PLACE FT	QT(J) SCF	3 LAYERS SO SCF	PW PSIA	TME DAYS
1	1	3.	.34682079E 04	.20000000E 05	1295.0	.01
1	2	7.	.92485550E 04	.20000000E 05	1295.0	.01
1	3	9.	.72832371E 04	.20000000E 05	1295.0	.01
2	1	4.	.96585897E 04	.60000000E 05	1424.4	.03
2	2	12.	.27965439E 05	.60000000E 05	1424.4	.03
2	3	14.	.22375970E 05	.60000000E 05	1424.4	.03
3	1	6.	.18783526E 05	.12000000E 06	1420.6	.06
3	2	17.	.56080525E 05	.12000000E 06	1420.6	.06
3	3	21.	.45135950E 05	.12000000E 06	1420.6	.06
4	1	8.	.30836738E 05	.20000000E 06	1408.8	.10
4	2	23.	.93606413E 05	.20000000E 06	1408.8	.10
4	3	27.	.75556851E 05	.20000000E 06	1408.8	.10
5	1	12.	.54790646E 05	.36000000E 06	1397.3	.18
5	2	31.	.16868676E 06	.36000000E 06	1397.3	.18
5	3	37.	.13652259E 06	.36000000E 06	1397.3	.18
6	1	14.	.81525728E 05	.54000000E 06	1386.0	.27
6	2	38.	.25319030E 06	.54000000E 06	1386.0	.27
6	3	45.	.20528396E 06	.54000000E 06	1386.0	.27
7	1	18.	.13173417E 06	.88000000E 06	1376.0	.44
7	2	49.	.41285665E 06	.88000000E 06	1376.0	.44
7	3	58.	.33540915E 06	.88000000E 06	1376.0	.44
8	1	22.	.19323516E 06	.13000000E 07	1366.0	.65
8	2	60.	.61019378E 06	.13000000E 07	1366.0	.65
8	3	71.	.49657109E 06	.13000000E 07	1366.0	.65
9	1	26.	.25135079E 06	.17000000E 07	1357.8	.85
9	2	69.	.79822654E 06	.17000000E 07	1357.8	.85
9	3	82.	.65042270E 06	.17000000E 07	1357.8	.85
10	1	34.	.43920251E 06	.30000000E 07	1349.8	1.50
10	2	92.	.14095337E 07	.30000000E 07	1349.8	1.50
10	3	110.	.11512638E 07	.30000000E 07	1349.8	1.50
11	1	49.	.86714341E 06	.60000000E 07	1336.4	3.00
11	2	132.	.28212966E 07	.60000000E 07	1336.4	3.00
11	3	157.	.23115599E 07	.60000000E 07	1336.4	3.00
12	1	63.	.14271936E 07	.10000000E 08	1320.3	5.00
12	2	171.	.47054951E 07	.10000000E 08	1320.3	5.00
12	3	204.	.38673116E 07	.10000000E 08	1320.3	5.00
13	1	75.	.19780014E 07	.14000000E 08	1309.3	7.00
13	2	204.	.65911441E 07	.14000000E 08	1309.3	7.00
13	3	244.	.54308545E 07	.14000000E 08	1309.3	7.00
14	1	79.	.19722867E 07	.14000000E 08	1220.4	8.00
14	2	214.	.65920662E 07	.14000000E 08	1220.4	8.00
14	3	256.	.54356471E 07	.14000000E 08	1220.4	8.00
15	1	82.	.19673834E 07	.14000000E 08	1152.7	10.00
15	2	222.	.65928416E 07	.14000000E 08	1152.7	10.00
15	3	266.	.54397748E 07	.14000000E 08	1152.7	10.00
16	1	83.	.19650160E 07	.14000000E 08	1123.2	12.00
16	2	226.	.65932102E 07	.14000000E 08	1123.2	12.00
16	3	270.	.54417739E 07	.14000000E 08	1123.2	12.00
17	1	87.	.25156796E 07	.18000000E 08	1270.2	13.00
17	2	237.	.84786588E 07	.18000000E 08	1270.2	13.00
17	3	283.	.70056607E 07	.18000000E 08	1270.2	13.00
18	1	98.	.35998854E 07	.26000000E 08	1371.3	15.00
18	2	270.	.12252117E 08	.26000000E 08	1371.3	15.00
18	3	323.	.10147995E 08	.26000000E 08	1371.3	15.00
19	1	110.	.46687699E 07	.34000000E 08	1400.1	17.00
19	2	304.	.16027514E 08	.34000000E 08	1400.1	17.00
19	3	365.	.13303713E 08	.34000000E 08	1400.1	17.00
20	1	122.	.57244120E 07	.42000000E 08	1406.2	19.00
20	2	337.	.19804373E 08	.42000000E 08	1406.2	19.00
20	3	405.	.16471211E 08	.42000000E 08	1406.2	19.00
21	1	127.	.61120331E 07	.45000000E 08	1386.8	20.00
21	2	353.	.21221590E 08	.45000000E 08	1386.8	20.00
21	3	423.	.17666376E 08	.45000000E 08	1386.8	20.00
22	1	137.	.68866779E 07	.51000000E 08	1365.4	22.00
22	2	380.	.24055922E 08	.51000000E 08	1365.4	22.00
22	3	456.	.20057399E 08	.51000000E 08	1365.4	22.00
23	1	149.	.80417245E 07	.60000000E 08	1348.4	25.00
23	2	415.	.28307796E 08	.60000000E 08	1348.4	25.00
23	3	499.	.23650479E 08	.60000000E 08	1348.4	25.00
24	1	152.	.80249804E 07	.60000000E 08	1300.8	26.00
24	2	426.	.28309490E 08	.60000000E 08	1300.8	26.00
24	3	512.	.23665528E 08	.60000000E 08	1300.8	26.00
25	1	160.	.79913693E 07	.60000000E 08	1208.2	30.00
25	2	447.	.28312765E 08	.60000000E 08	1208.2	30.00
25	3	538.	.23695864E 08	.60000000E 08	1208.2	30.00
26	1	162.	.86422972E 07	.65000000E 08	1257.2	31.00
26	2	453.	.30673551E 08	.65000000E 08	1257.2	31.00
26	3	546.	.25684149E 08	.65000000E 08	1257.2	31.00
27	1	168.	.99280884E 07	.75000000E 08	1319.6	33.00
27	2	471.	.35396561E 08	.75000000E 08	1319.6	33.00
27	3	568.	.29675348E 08	.75000000E 08	1319.6	33.00
28	1	175.	.11199884E 08	.85000000E 08	1356.9	35.00
28	2	492.	.40120597E 08	.85000000E 08	1356.9	35.00
28	3	593.	.33679515E 08	.85000000E 08	1356.9	35.00
29	1	183.	.12459483E 08	.95000000E 08	1378.9	37.00
29	2	515.	.44845354E 08	.95000000E 08	1378.9	37.00
29	3	621.	.37695154E 08	.95000000E 08	1378.9	37.00
30	1	186.	.12825044E 08	.98000000E 08	1367.4	38.00
30	2	526.	.46263600E 08	.98000000E 08	1367.4	38.00
30	3	634.	.38911353E 08	.98000000E 08	1367.4	38.00

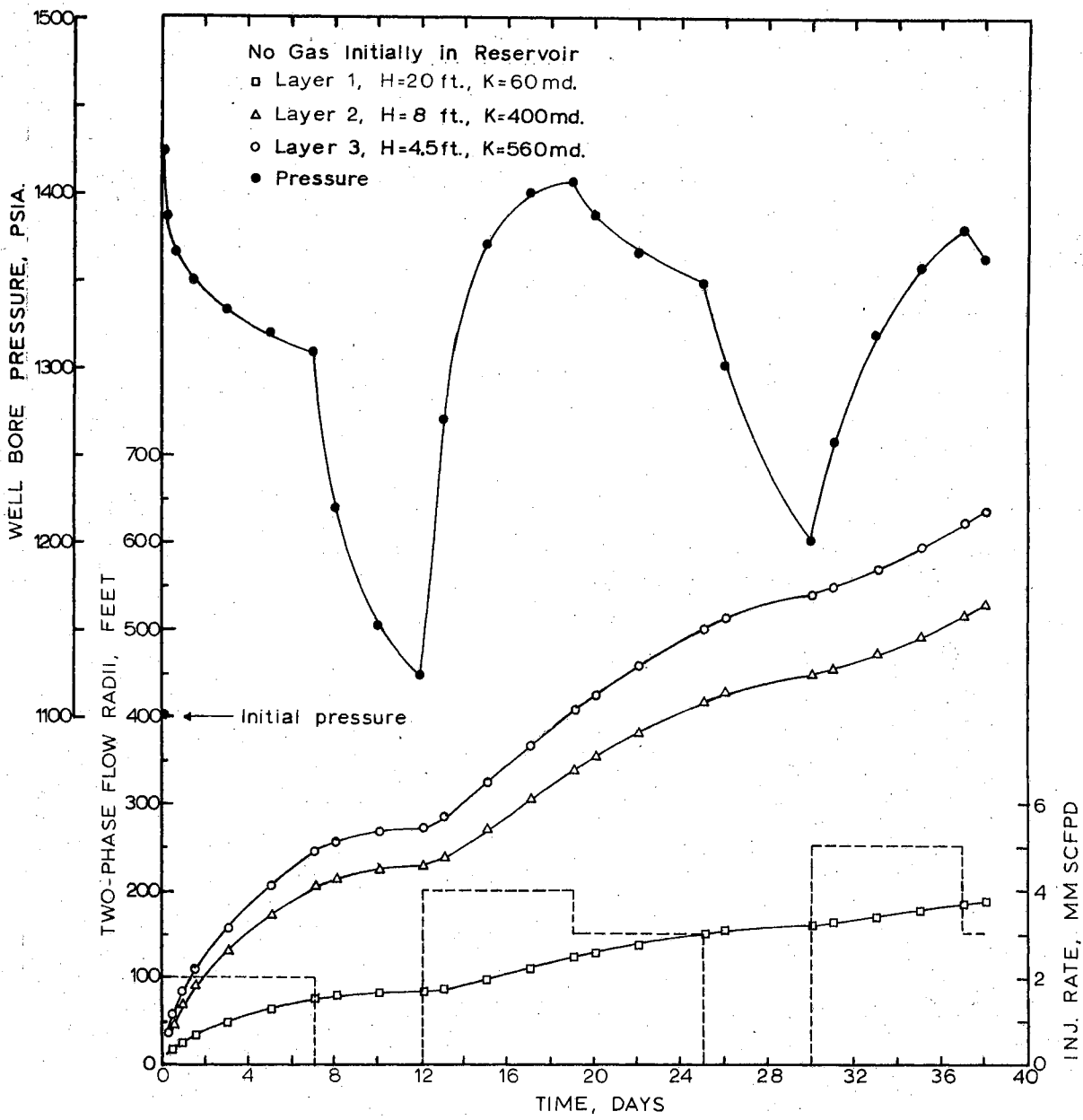


Figure 18. Predicted Gas Zone Performance, Case I.



Case II had the same input data as the first example, with the following exceptions: 1) the relative permeability curves used were for the second, rather than first, drainage cycle, 2) an initial gas saturation of 22 percent existed in all layers inside these radii: layer 1, 186 feet; layer 2, 526 feet; layer 3, 634 feet. Care must be taken to see that the initial radii, initial gas saturation, and amount of gas in place coincide accurately. Slide rule accuracy is not acceptable to the program.

Figure 19 shows well bore pressure and two-phase flow zone radii for Case II. When injection began, well bore pressure increased much more slowly than in Case I. This was due to the more rapid building of the two-phase flow zones and the compressibility of gas already in place.

In order to determine whether or not it is necessary to calculate the division of flow among the layers as suggested in Chapter III, a comparison was made of the amount of gas in each layer as predicted by the frontal drive technique and as predicted by simple division of flow on a permeability times thickness basis. The results are shown in Figures 20 and 21. A simple permeability times thickness division of flow showed too much gas entering the low permeability layer and not enough entering the ones of high permeability.

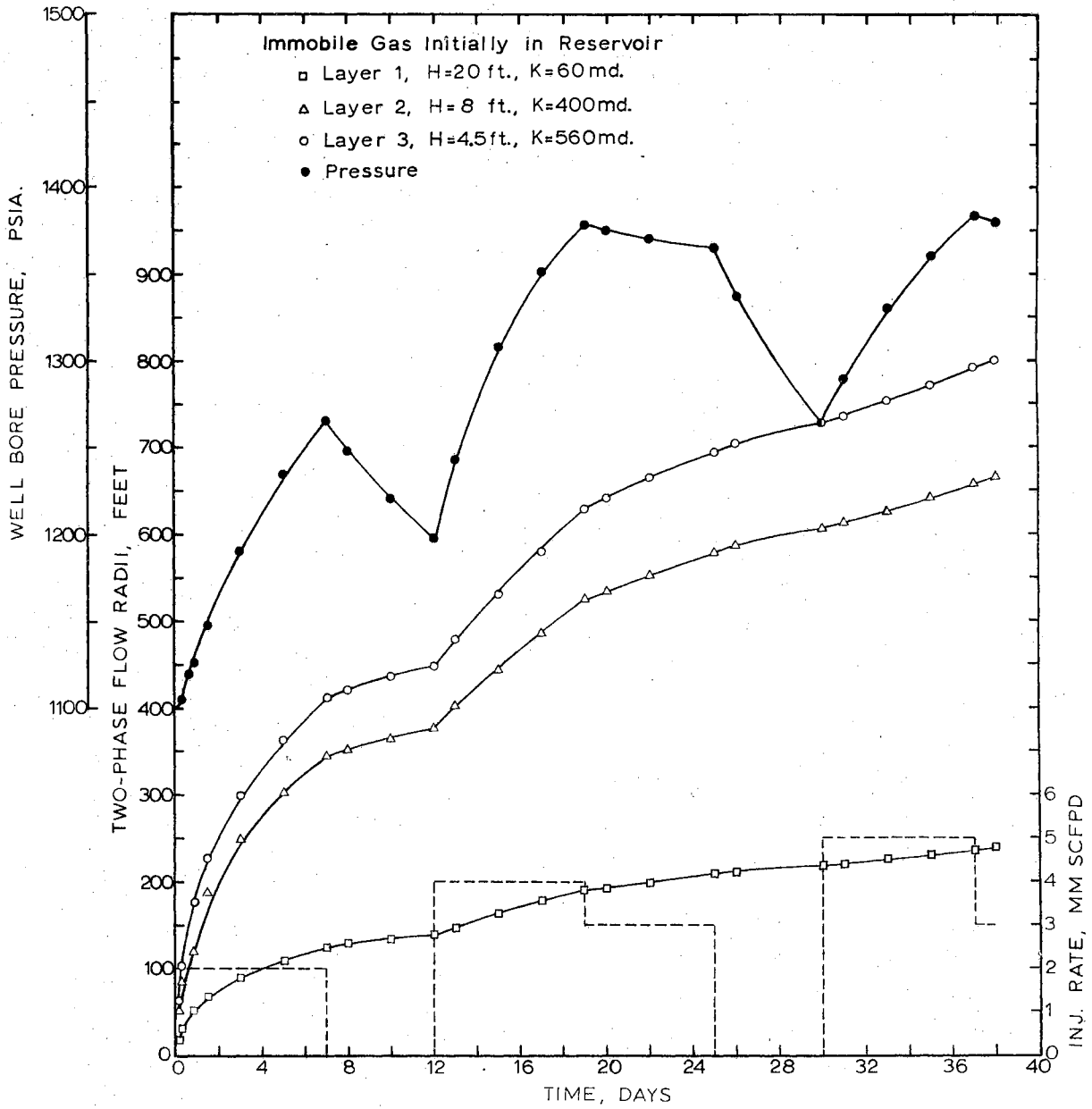


Figure 19. Predicted Gas Zone Performance, Case II.

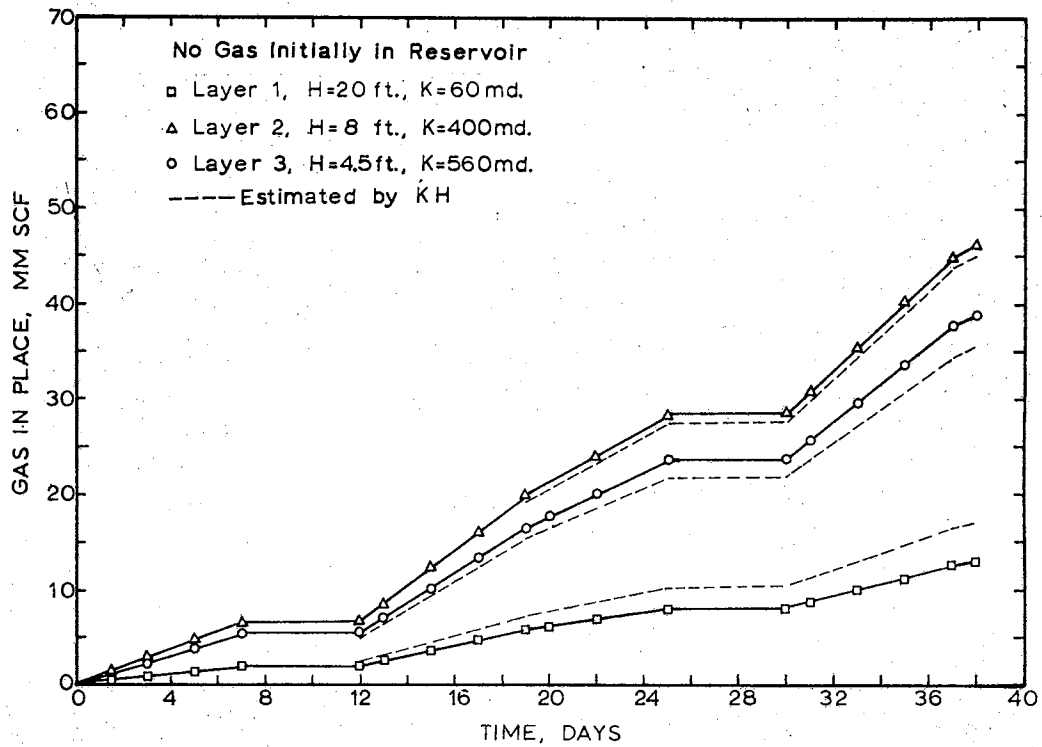


Figure 20. Distribution of Gas Among the Layers, Case I.

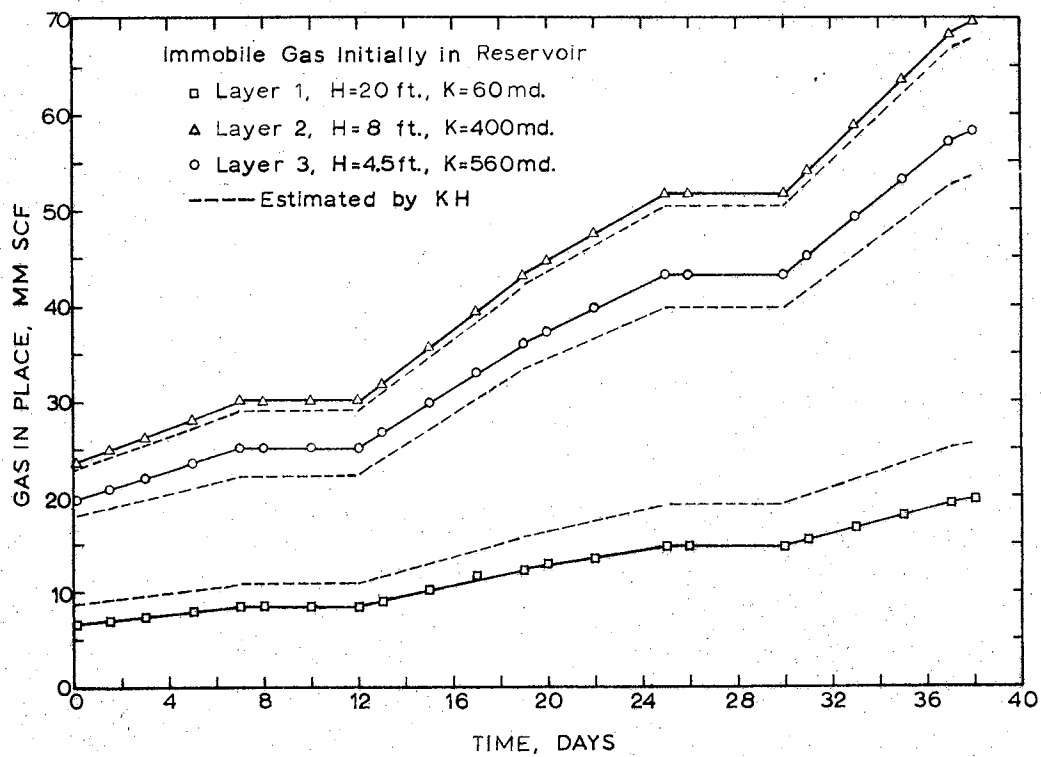


Figure 21. Distribution of Gas Among the Layers, Case II.

## CHAPTER VI

### SUMMARY AND CONCLUSIONS

Previously used methods of predicting water flood performance and reserves of stratified reservoirs have generally given estimates which were too optimistic. The method presented in this thesis utilizes frontal drive theory to avoid assuming piston-like displacement. For the example problem it gave much more conservative predictions than the other methods used, thus more nearly approaching published information on actual water flood performances. As presented, the method is not rigorous enough to have never-failing accuracy; however, it is believed to be a marked improvement over previous methods. The reliability of its predictions can be proved or disproved only by comparison with the actual results of water flooding many reservoirs.

Previously no method has been available for predicting the behavior of a stratified aquifer upon the injection of gas. The method presented herein is based upon one which was successful in predicting actual results for a single-layer radial one-well gas storage reservoir. It is severely limited by the assumption of a single-well radial system, which could exist only during the initial development of a new gas storage reservoir. It is believed that by applying various initial conditions, engineers will be able to obtain qualitative information which will be quite useful in developing stratified reservoirs to their maximum storage

capacity. This multi-layer approach will almost certainly be modified and improved.

In conclusion, the writer considers this study to have made a small but significant contribution to the better understanding of reservoir performance.

## CHAPTER VII

### RECOMMENDATIONS FOR FUTURE STUDY

There exists a great need for better methods of describing two-phase flow phenomena in heterogeneous reservoirs, including stratified reservoirs.

In regard to water flooding, techniques need to be developed to better take into account reservoir geometry. Perhaps the geometry of each individual layer should be considered. An approach allowing cross flow between the layers would be quite useful. One simple and recommended modification of the given computer programs is a change to allow production to begin as soon as fill-up occurs in the most permeable layer rather than when fill-up occurs in all layers. Also a modification to allow the existence of a trapped gas saturation in the oil bank would make the programs more flexible. The advent of tertiary and more exotic secondary recovery processes will certainly bring complex multi-phase flow problems.

In regard to gas storage in aquifers, many extensions of and additions to the present knowledge of two-phase flow are needed. The method presented herein of predicting two-phase behavior in stratified reservoirs could be expanded upon in several ways such as: 1) inclusions of cyclic effects with relative permeability hysteresis, 2) assuming the stratification continues throughout the aquifer, 3) allowing the layers

to have different relative permeability characteristics and separate aquifers in order to study the possibility of using a single well bore for injection and withdrawal from more than one formation without mechanically separating the flow, 4) inclusion of capillary and gravitational effects and 5) allowing cross-flow between the layers.

A technique is urgently needed to represent a multi-well system for gas injection and withdrawal. Perhaps a grid approach similar to that described by Blair and Peaceman (1) for a gas-oil system might prove fruitful.

Since the results of any calculation are no better than the input data used, it is evident that more and better relative permeability data will be needed. Further refinement of experimental techniques or the development of reliable correlations is needed to supply improved relative permeability data.

#### SELECTED BIBLIOGRAPHY

1. Blair, P. M. and D. W. Peaceman. "An Experimental Verification of a Two-Dimensional Technique for Computing Performance of Gas-Drive Reservoirs," SPE Journal (March, 1963) 3, No. 1, 19.
2. Buckley, S. E. and M. C. Leverett. "Mechanism of Fluid Displacement in Sands," Trans. AIME (1942) 146, 149.
3. Collins, R. E. Flow of Fluid Through Porous Materials, Reinhold, New York, (1961), 114.
4. Craft, B. C. and M. F. Hawkins. Applied Petroleum Reservoir Engineering, Prentice-Hall, Englewood Cliffs, N. J. (1959), 314.
5. Craig, F. F., T. M. Geffen, and R. A. Morse. "Oil Recovery Performance of Pattern Gas or Water Injection Operations from Model Tests," Trans. AIME (1955) 204, 7.
6. Dyes, A. B., B. H. Caudle, and R. A. Erickson. "Oil Production After Breakthrough as Influenced by Mobility Ratio," Trans. AIME (1954) 201, 240.
7. Dykstra, H. and R. L. Parsons. "The Prediction of Oil Recovery by Water Flood," Secondary Recovery of Oil in the United States, American Petroleum Institute, New York (1950).
8. Guerrero, E. T. and R. C. Earlougher. "An Analysis and Comparison of Five Methods Used to Predict Water-Flood Reserves and Performance," Producers Monthly (March, 1961) 26, 4.
9. Hurst, W. and A. F. Van Everdingen. "The Application of Laplace Transformation to Flow Problems in Reservoirs," Trans. AIME (1949) 186, 305.
10. Katz, D. L. et al. Handbook of Natural Gas Engineering, McGraw-Hill, New York (1959), 112.
11. Pirson, S. J. Oil Reservoir Engineering, McGraw-Hill, New York (1958), 389.



12. Stiles, W. E. "Use of Permeability Distribution in Water Flood Calculations," Trans. AIME (1949) 186, 9.
13. Welge, H. J. "A Simplified Method for Computing Oil Recovery by Gas or Water Drive," Trans. AIME (1952) 195, 91.
14. Woods, E. G. and A. G. Comer. "Saturation Distribution and Injection Pressure for a Radial Gas Storage Reservoir," Trans. AIME (1962) 225, 1389.
15. Woods, E. G. An Investigation of Cyclic, Immiscible Two-Phase Flow in Porous Media, Ph.D. Dissertation, Oklahoma State University, Stillwater, Oklahoma (May, 1963).

APPENDIX

LIST OF SYMBOLS FOR THE TEXT

A	Cross sectional area.
C	Compressibility of the aquifer, $\text{psi}^{-1}$ .
$Ei(X)$	Exponential integral of X.
$f_w$	Fractional flow of water at a given saturation.
$f_g$	Fractional flow of gas at a given saturation.
$F_w$	Producing water cut at reservoir conditions.
$F_{ws}$	Producing water cut at surface conditions.
g	Gravitational constant.
$h_j$	Thickness of layer j, ft.
$h_a$	Thickness of the aquifer, ft.
$K_a$	Effective permeability of the aquifer, md.
$K_j$	Absolute permeability of layer j, md.
$K_o$	Effective permeability to oil, md.
$K_w$	Effective permeability to water, md.
$k_{rg}$	Relative permeability to gas.
$k_{ro}$	Relative permeability to oil.
$k_{rw}$	Relative permeability to water.
L	Length.
$\bar{M}_i$	Average total relative fluid mobility in shell i, $\text{cp}^{-1}$ .
p	Average pressure in the two-phase flow region, psia.
$p_a$	Pressure at the exterior boundary of the "incompressible core", psia.

$P_c$	Capillary pressure.
$p_e$	Undisturbed aquifer pressure, psia.
$P_o$	Pressure in the oil phase.
$P_w$	Well bore pressure, psia.
$P_w$	Pressure in the water phase.
$q$	Total flow rate. <sup>1</sup>
$q_d$	Pseudo-dimensionless flow rate, psi.
$q_j$	Total flow rate in layer j.
$q_o$	Oil flow rate.
$q_w$	Water flow rate.
$Q_j$	Cumulative amount of gas layer j, SCF.
$r_{bj}$	Radius of the two-phase flow region in layer j, ft.
$r_{bmj}$	Maximum previous radius of the two-phase flow region in layer j, ft.
$R_d$	Dimensionless radius.
$r_s$	Radius of constant saturation S, ft.
$r_w$	Well bore radius, ft.
$S_o$	Oil saturation.
$S_w$	Water saturation.
$\bar{S}_g$	Average gas saturation in the two-phase flow region.
$S_{gi}$	Gas saturation between $r_b$ and $r_{bm}$ .
$T$	Reservoir temperature, °R.
$T_{bsc}$	Base temperature for gas measurements, °R.
$t$	Time, days.

---

<sup>1</sup>Note: Flow rates used in connection with water flooding are in barrels per day while those used in gas storage are in cubic feet per day.

$t_d$	Dimensionless Time.
$W$	Width.
$X$	Distance.
$X_f$	Distance to the flood front.
$Z$	Gas deviation factor.
$\alpha$	The angle at which fluid flow deviates from horizontal (downward positive).
$\Delta P_{ic}$	Pressure differential across the "incompressible region", psia.
$\Delta P_{tpj}$	Pressure differential across the two-phase flow portion of layer $j$ , psi.
$\Delta P_{wj}$	Pressure differential across the single phase flow portion of layer $j$ , psi.
$\Delta P_{us}$	Pressure change at the internal radius of the unsteady state region, psi.
$\phi_a$	Porosity of the aquifer, fractional.
$\phi_j$	Porosity of layer $j$ , fractional.
$\rho_o$	Density of the oil.
$\rho_w$	Density of the water.
$R_j$	Flow resistance factor for layer $j$ .
$R_{tp}$	Flow resistance factor for the two-phase flow region.
$\mu_g$	Gas viscosity, cp.
$\mu_o$	Oil viscosity, cp.
$\mu_w$	Water viscosity, cp.

VITA

Elton Wayne Adams

Candidate for the Degree of

Master of Science

Thesis: APPLICATION OF FRONTAL DRIVE PRINCIPLES TO STRATIFIED  
RESERVOIRS

Major Field: Mechanical Engineering

Biographical:

Personal Data: Born July 14, 1939, in Lela, Oklahoma, the son  
of James R. and Hazel L. Adams.

Education: Graduated from Burbank High School, Burbank, Oklahoma,  
in 1957; received the Associate of Science degree from Northern  
Oklahoma Junior College, Tonkawa, Oklahoma, in May 1959; re-  
ceived the Bachelor of Science degree from Oklahoma State  
University, with a major in Mechanical Engineering, in May,  
1962; completed requirements for the Master of Science degree  
in April, 1964.

Experience: Employed by Kewanee Oil Company, Tulsa, Oklahoma, during  
summers of 1959, 1960, and 1961 as roustabout, pumper, and  
engineer's assistant. Employed by The Atlantic Refining  
Company, Oklahoma City, Oklahoma as engineering aide from June  
to September, 1962. Employed by Oklahoma State University,  
Mechanical Engineering Department from February to May, 1962  
and from September, 1962, to March, 1964, as part-time research  
assistant.

Professional Organizations: AIME Society of Petroleum Engineers,  
Engineer-in-Training, Oklahoma.